nature portfolio

Peer Review File

Unusual Diffusion of Chiral Active Brownian Particles in Deformable and Displaceable Media

Corresponding Author: Ms Luhui Ning

This file contains all reviewer reports in order by version, followed by all author rebuttals in order by version.

Version 0:

Reviewer comments:

Reviewer #1

(Remarks to the Author)
The authors study chiral active Brownian particles confined in an annular channel, with deformable and ring-shaped obstacles. Through experiments based on hexbug particles (active granular particles) and theory, the authors report a non-monotonic dependence of the particle diffusion coefficient on the area fraction of the obstacles.

The present paper is well-written and shows interesting results. The experimental setup is original and tackles an interesting topic that deserves publication in Communication Physics. Before I can recommend this paper for publication, the authors should answer my doubts (mainly on the theoretical analysis) and address my questions, which are listed below.

- The authors do not mention any details for the extraction of parameters. What is the method employed to extract the parameter in Table 1? The authors should add a section in the methods (mentioned in the main text) to add details on the parameter extraction.
- Related to the previous point, active particles are typically characterized by a self-propelled speed v_0, an angular velocity omega_0, a persistence time tau, which can be identified (in two dimensions) as the inverse of the effective rotational diffusion coefficient, and an effective translational diffusion coefficient. While I could agree that the translational diffusion coefficient could be small and irrelevant, we cannot say the same for the persistence time. Is the method employed to extract the parameters suitable to predict the value of the persistence time? The authors should estimate this time and calculate the corresponding persistence length.
- The previous point is relevant because, from Table 1, one can be tempted to say that the chosen robots have different angular velocities with almost constant speed, resulting in different orbital radii. From a measurement of the persistence time, I expect that different particles have almost the same persistence length.

- In the introduction or conclusion, the authors should mention other realizations of active granular particles showing circular motion, i.e. chiral:
* Vega Reyes, F., López-Castaño, M. A., & Rodríguez-Rivas, Á. (2022). Diffusive regimes in a two-dimensional chiral fluid. Communications Physics, 5(1), 256.
* Caprini, L., Abdoli, I., Marconi, U. M. B., & Löwen, H. (2025). Spontaneous self-wrapping in chiral active polymers. Newton 2025. DOI: 10.1016/j.newton.2025.100253

- The theoretical result (Eq.(3)) was first derived in the following paper:
* Van Teeffelen, S., & Löwen, H. (2008). Dynamics of a Brownian circle swimmer. Physical Review E—Statistical, Nonlinear, and Soft Matter Physics, 78(2), 020101.
The authors should also mention other papers where the theory of potential-free or confined chiral active particles has been considered:
* Sevilla, F. J. (2016). Diffusion of active chiral particles. Physical Review E, 94(6), 062120.
* Caprini, L., & Marconi, U. M. B. (2019). Active chiral particles under confinement: Surface currents and bulk accumulation phenomena. Soft Matter, 15(12), 2627-2637.
* Joshi, J., & Mishra, S. (2025). Analytical Theory of Chiral Active Particle Transport in a Fluctuating Density Field. arXiv preprint arXiv:2508.15366.ù
* Caprini, L., Löwen, H., & Marconi, U. M. B. (2023). Chiral active matter in external potentials. Soft Matter, 19(33), 6234-6246.

- The non-monotonic dependence of the diffusion coefficient with density has already been observed in numerical simulations, for instance, in
* Van Roon, D. M., Volpe, G., da Gama, M. M. T., & Araújo, N. A. (2022). The role of disorder in the motion of chiral active particles in the presence of obstacles. Soft Matter, 18(36), 6899-6906.
The authors should comment on this.

- In the theoretical prediction (3), the authors state that tau_r is the rotational relaxation time given by the rotational friction coefficient gamma_r and the temperature T. This is not correct. Indeed, tau_r is the particle persistence time, which for a single particle is an intrinsic parameter of the dynamics. This time is often identified as the autocorrelation time of the orientation or through the mean-square displacement, specifically as the time needed to approach a diffusive behavior from the ballistic behavior induced by the activity. In addition, the authors should clarify the equalities, gamma_r=t_m/t_tot and gamma_t=v_0/v, adding more details and explaining why this is true.

- In this paper, theoretical predictions are not derived. The authors should specify that they have developed a scaling argument.

- The authors report some empirical functions that capture the behavior of the functions gamma_r and gamma_t. The authors should remove this fitting analysis: there is no point in these predictions, which are not supported by theory and therefore do not add anything to the present paper.

Minor points:
- page 1 "hyperuniform" --> "hyperuniformity"
- page 1. "In this Letter" --> "In this paper"

Reviewer #2

(Remarks to the Author)
This manuscript studies the motion of a CAP in a system of deformable and displaceable obstacles on a vibrating stage. This work serves as a valuable complement to previous studies on particle motion in rigid and fixed obstacle arrays. It is known that particle motion can be suppressed by obstacles and promoted by 1D-like channels between obstacles, leading to a non-monotonic dependence of particle diffusion on obstacle density. The authors successfully reproduce this expected behavior and further demonstrate that diffusion at certain intermediate obstacle densities can be up to 100 times higher than in the obstacle-free case. While the findings are interesting, the authors should address the following major points before I can recommend publication:

1. The function q(θ) in Eq. (2) contains an arbitrarily defined parameter b. Why not replace Q(t) with a standard autocorrelation function of the particle's orientation, which would be unambiguous with a clear meaning?
2. The specific criterion used to identify "trapped" and "migration" states should be explicitly defined and provided in the manuscript.
3. The rationale behind the metric v^2 t_m/(v_0^2 t_tot) needs to be explained. Please clarify why this specific combination is chosen to capture the combined effects.
4. The origin and derivation of Eqs. (4) and (5) should be stated. Please provide a reference or derivation.
5. The term "deformable" is highlighted in the title, abstract, and discussion, but the degree of deformability is not quantified. A rough estimate of the obstacle deformation under the given particle activity is needed. Furthermore, some obstacles in the videos appear non-circular. Could particle collisions induce irreversible (plastic) deformation? The potential effects of both deformation and non-circular shape should be discussed.
6. Are the two videos under the same obstacle density? Captions for both videos are missing.

Minor Comments:
1. Given the relatively small system size, are boundary effects pronounced? It would be straightforward to study a larger system to confirm the results are not influenced by finite-size effects.
2. Please clarify if the measured angular displacement Δθ can exceed 2π.

Reviewer #3

(Remarks to the Author)
The motion of self-propelled particles interacting with soft obstacles is investigated in annular confinement conditions. The experimental part of the study is performed with commercial Hexbugs whose legs are modified to perform helical motions with variable orbital radius. Results are compared with an analytical description partly developed for dense active matter systems and here adapted with an empirical estimation of the relevant functions. The transition between trapping and migrating has been recently described for active polymerlike worms interacting with and movable obstacles (PRL 134, 128303 (2025), arXiv:2503.15755). In spite of the differences, it seems that the transition between trapping and migrating is a common property of both systems. In the title and the overall manuscript the system under study is described as a paradigm of chiral active particles. Meanwhile, it is not so clear to me that the chirality of the particles plays a relevant role in the actual mechanism described here.

I like this work, and I am certain that a modified version of this manuscript deserves publication, but I am not sure about its suitability for Communication Physics.

I have various other comments that the authors might want to consider:

1.- In the introduction, no distinction is made between chiral active Brownian particles and rotors. CAP are then referred as having both self-propulsion and autonomous rotation, which applies to their system but not to rotors. The authors could explain if this crucial conceptual difference has an effect in the observations they made.

2.- In my opinion, since Figures 6b and 7a,c refer to the reference motion, it would be more clear if discussed much earlier, maybe directly after Fig 2 or even before.

3.- The ratio between the Hexbug size and the orbital ratio is not discussed. And maybe more relevant the comparison of the length of both the Hexbug and its trajectory with the obstacles size might play a crucial role.

4.- How much do the results hinge on the softness of the obstacles? Could experiments be performed also with more rigid objects, such as thin rings?

5.- Eq.(3) seems to be obtained in the obstacle-free space case, looking at the trajectories in Fig.7a it seems questionable.

6.- Then the applicability of Eq.(3) is extended to complex media, which is not obvious either, also regarding the trajectories in Fig.7. The authors should extensively comment on this.

7.- The measurement of diffusion is of central importance to this work, but judging from the results in Fig2a it is not completely clear tat the linear regime has been properly reached. It could be that the measurements are too short, or that there is another mechanism preventing this. Maybe plot MSD/t vs. t would help in this respect, and also to clarify the origin of the really large error bars in Fig2b.

8.- The influence of the employed confinement geometry is also barely discussed.
8a -- Would the results be very different if the confinement would be simply circular, $R_{in}=0$,
8b -- or if there would not be any confinement, $r_{out} \gg r$?
8c -- for $r \simeq R_{in}$ could there be some sort of particular enhancement ?
8d -- could experiments in other geometries be performed ?
8e -- could some more insights on how the results would translate to a different geometry be provided ?

9.- What is the advantage of analyzing the self-overlap function instead of the more traditional orientation autocorrelation function ?

10.- How are F_d and T_D evaluated ?

11.- In line 177 the authors make an unclear connection between the system heterogeneity and to supercooled liquids.

12.- The migration time, first appearing in line 192 is not defined before and not afterwards.

13.- I guess that the velocities are measured from the MSD (please specify), but how are the migration times obtained ? I understand that the manuscript specifies migration time and relaxation times as two different quantities.

14.- The four plots in Fig 4 might be more informative if they would all be presented in a single plot. The functions used to fit Fig.4b should be specified in the caption.

15.- The fits performed in Fig. 4b could be also extended to the other 4 sets of parameters. Is there a reason why this is not done? Would the fitted values be very different ?

16.- I am not sure I properly understand, but it seems that Fig. 5b corresponds to the fits obtained and already shown in Fig 4b. If I am right, I am not sure why this is repeated here. Why are symbols used in the inset and not in the main plot? And would it be possible to plot the values in Fig 2b together with the relation obtained from the velocities and migration times.

17.- The so-called prediction in Eq.(6) provides the behavior of the diffusion coefficient as the ratio of two frictions which are obtained by an empirical fitting. The great agreement in Fig 5c has some value, but provides somehow recursive information. Unless I am missing something.

18.- Although the whole manuscript focusses on chiral particles, Fig.3b implies that the effect of chirality plays a subdominant role. The importance of chirality is not so easy to appreciate since results are plotted in terms of D/D_0, where D_0 is different for different r.

19.- Is the transition between trapped and migration states similar to that described for self-propelled polymers in a complex media (PRL 134, 128303 (2025))

In summary, the authors present a study of a very particular system and particular conditions and it should be more clear how the results here discussed can be applied to other systems.

Reviewer #4

(Remarks to the Author)
I co-reviewed this manuscript with one of the reviewers who provided the listed reports. This is part of the Communications Physics initiative to facilitate training in peer review and to provide appropriate recognition for Early Career Researchers who co-review manuscripts.

Version 1:

Reviewer comments:

Reviewer #1

(Remarks to the Author)
The authors have addressed my main comments in the reply to the Referees and have modified the manuscript accordingly. As I have stated in my previous report, the authors present an experimental setup that allows them to tackle an interesting problem and find interesting results.

As a consequence, I believe that this paper can be published in its current form.

Reviewer #2

(Remarks to the Author)
My questions have been satisfactorily addressed. I recommend the publication.

Reviewer #3

(Remarks to the Author)
The authors have submitted a revised and significantly enlarged version of the work,
as can be seen by the pages extra of the main manuscript and 10 of the supplementary material.
The answers to the comments were very complete and satisfactory. Overall, I think that the manuscript
has largely gained in clarity and completeness, and it will become a reference work in the field.
Therefore, I recommend it now for publication in for Communication Physics.

I would like still to add this few comments for the optional consideration of the authors.

- Although complete, I found the answers to the comments excessively long and repetitive,
and at some points they gave the impression that quite some AI was used.

- Regarding points 18 & 19. I am not completely convinced yet about the relevance of chirality in the
coexistence of trapped and migratory dynamical states. Here, it can be true that
the interactions between the chirality-driven circular motion and obstacles enables the
transitions between the two states, but this could have as well happened due to the interaction
of a random active motion and a disordered media.

- The authors adapt the effective diffusion coefficient of CABP from the literature and apply it
to the angular MSD they measure. However, it is not quite clear how they can adapt the 2D result
for the CABP to their 1D case, since, e.g., the dimensions of Eq.(3) is not 1/s but cm^2/s,
which cannot be consistent with the MSD definition. The authors should verify that the omission
of the radial coordinate here is consistent.

- Regarding point 7 of referee 1. To extrapolate the definition of temperature from micrometer
systems to this centimeter systems is not completely straightforward, and that the use of other
concepts like particle persistence time might be more appropriate. Equations (4) to (7) make
use of microscopic definitions, including temperature, which cancels out in the end in Eq.(8)

Reviewer #4

(Remarks to the Author)
I co-reviewed this manuscript with one of the reviewers who provided the listed reports. This is part of the Communications Physics initiative to facilitate training in peer review and to provide appropriate recognition for Early Career Researchers who co-review manuscripts.

Response to the comments from Reviewer 1

General comment:

The authors study chiral active Brownian particles confined in an annular channel, with deformable and ring-shaped obstacles. Through experiments based on hexbug particles (active granular particles) and theory, the authors report a non-monotonic dependence of the particle diffusion coefficient on the area fraction of the obstacles.

The present paper is well-written and shows interesting results. The experimental setup is original and tackles an interesting topic that deserves publication in Communication Physics. Before I can recommend this paper for publication, the authors should answer my doubts (mainly on the theoretical analysis) and address my questions, which are listed below.

Response: We thank the reviewer for recognizing the relevance of our work and for the constructive comments. All questions and concerns have been addressed in detail, and corresponding revisions have been incorporated to improve the manuscript.

Comment (1): The authors do not mention any details for the extraction of parameters. What is the method employed to extract the parameter in Table 1? The authors should add a section in the methods (mentioned in the main text) to add details on the parameter extraction.

Response (1): We thank the reviewer for raising this important point. In the revised manuscript, a detailed description for the extraction of parameters reported in Table 1 has been added to the Methods section. Briefly, for chiral active Brownian particles (CABPs) moving in free space, the translational velocity v_0 is obtained from frame-to-frame displacements divided by the corresponding time interval and averaged over the entire trajectory. The angular velocity ω_0 is extracted by tracking the particle's orientation angle in each frame, calculating the angular displacement per unit time, and averaging over time. The orbital radius is then defined as $r = v_0/\omega_0$, and the rotation period as T=$2\pi/\omega_0$.

Text changes:

1. Page 7, right column, the section of Methods

At the end of the second paragraph, we added the following sentences: “For CABP moving in free space, the mean translational velocity v_0 was obtained by averaging the displacement between consecutive frames divided by the frame interval over the entire trajectory. The angular velocity ω_0 was determined by tracking the particle orientation in each frame and averaging the angular increment per unit time. The orbital radius was defined as $r = v_0/\omega_0$, and the rotation period as $T = 2\pi/\omega_0$. The effective rotational diffusion coefficient D_r was extracted from the mean squared angular displacement (MSAD), $\langle[\varphi(t_0+t)-\varphi(t_0)]^2\rangle = \omega^2t^2 + 2D_rt$ [Supplementary Materials], where $\varphi(t)$ denotes the orientation angle of the particle’s major axis [Soft Matter 12, 4584 (2016)]. The persistence time was then defined as $\tau_r = 1/D_r$ [Soft Matter 19, 6234 (2023)], and the corresponding persistence length as $l = v_0\tau_r$.”

Comment (2): Related to the previous point, active particles are typically characterized by a self-propelled speed v_0, an angular velocity ω_0, a persistence time τ_r, which can be identified (in two dimensions) as the inverse of the effective rotational diffusion coefficient, and an effective translational diffusion coefficient. While I could agree that the translational diffusion coefficient could be small and irrelevant, we cannot say the same for the persistence time. Is the method employed to extract the parameters suitable to predict the value of the persistence time? The authors should estimate this time and calculate the corresponding persistence length.

Response (2): We thank the reviewer for this helpful suggestion. In the revised manuscript, the persistence time and the corresponding persistence length are explicitly estimated using a standard approach. The effective rotational diffusion coefficient D_r is extracted from the mean squared angular displacement (MSAD), $\langle[\varphi(t_0+t)-\varphi(t_0)]^2\rangle = \omega^2t^2 + 2D_rt$ [Fig. R1], where $\varphi(t)$ denotes the orientation angle of the particle’s major-axis [Soft Matter 12, 4584 (2016)]. The persistence time is then obtained as $\tau_r = 1/D_r$ in two-dimensional system [Soft Matter 19, 6234 (2023)], and the corresponding persistence length is calculated as $l = v_0\tau_r$, with v_0 measured in free space. The extracted persistence time and corresponding persistence length for all chiral active Brownian particles have been included in the revised manuscript, and a detailed description of the parameter-extraction procedure has been added to the Methods section.

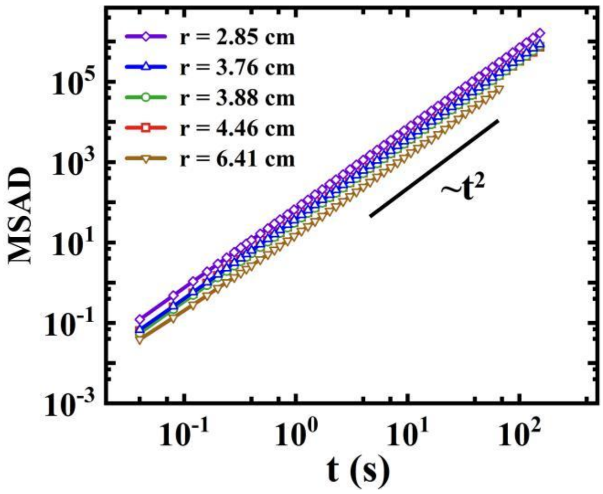

Fig. R1. The MSAD of five particles as a function of delay time *t* without soft-ring obstacles.

r (cm)	2.85	3.76	3.88	4.46	6.41
D_r (/s)	0.39±0.095	0.24±0.053	0.14±0.023	0.24±0.064	0.27±0.071
τ_r (s)	2.56	4.17	7.14	4.17	3.70
l (cm)	61.44±2.4	97.54±4.6	40.91±5.0	108.9±2.5	92.32±2.8

TABLE R1: Parameters of five Hexbugs used in the experiments. r, D_r, τ_r, and l represent the orbital radius, the rotational diffusion coefficient, the persistence time, and the persistence length of CAPBs in free space.

Text change:

1. Page 2, right column, Table 1

It was:

Robot	Orbital radius r (cm)	Angular velocity ω_0(s^{-1})	velocity v_0(cm/s)	Cycle period $T = \frac{2\pi}{\omega_0}$ (s)
1	2.85	8.43±0.24	24.04±0.94	0.74
2	3.76	6.23±0.21	23.39±1.11	1.01
3	3.88	5.73±0.13	22.28±0.70	1.10
4	4.46	5.85±0.21	26.12±0.61	1.07
5	6.41	3.89±0.28	24.95±0.75	1.61

TABLE 1: Parameters of five Hexbug robots used in the experiments. r, ω_0, and v_0 represent the orbital radius, the angular and translational velocity of CAPs in the absence of obstacles.

New reads:

Robot	1	2	3	4	5
R (cm)	2.85	3.76	3.88	4.46	6.41
v_0 (cm/s)	24.04±0.94	23.39±1.11	22.28±0.70	26.12±0.61	24.95±0.75
ω_0 (s^{-1})	8.43±0.24	6.23±0.21	5.73±0.13	5.85±0.21	3.89±0.28
T (s)	0.74	1.01	1.10	1.07	1.61
D_r (s^{-1})	0.39±0.095	0.24±0.053	0.14±0.023	0.24±0.064	0.27±0.071
τ_r (s)	2.56	4.17	7.14	4.17	3.70
l (cm)	61.44±2.4	97.54±4.6	40.91±5.0	108.9±2.5	92.32±2.8

TABLE 1: Parameters of five Hexbugs used in the experiments. r, v_0, ω_0, T, D_r, τ_r, and l represent the orbital radius, the translational velocity, the angular velocity, the cycle period, the rotational diffusion coefficient, the persistence time, and the persistence length of CABPs in the absence of obstacles.

2. Page 7, right column, the section of Methods

At the end of the second paragraph, we added the following sentences: "For CABP moving in free space, the mean translational velocity v_0 was obtained by averaging the displacement between consecutive frames divided by the frame interval over the entire trajectory. The angular velocity ω_0 was determined by tracking the particle orientation in each frame and averaging the angular increment per unit time. The orbital radius was defined as $r = v_0/\omega_0$, and the rotation period as $T = 2\pi/\omega_0$. The effective rotational diffusion coefficient D_r was extracted from the mean squared angular displacement (MSAD), $\langle[\varphi(t_0+t)-\varphi(t_0)]^2\rangle = \omega^2 t^2 + 2D_r t$ [Supplementary Materials], where $\varphi(t)$ denotes the orientation angle of the particle's major axis [Soft Matter 12, 4584 (2016)]. The persistence time was then defined as $\tau_r = 1/D_r$ [Soft Matter 19, 6234 (2023)], and the corresponding persistence length as $l = v_0\tau_r$."

Comment (3): The previous point is relevant because, from Table 1, one can be tempted to say that the chosen robots have different angular velocities with almost

constant speed, resulting in different orbital radii. From a measurement of the persistence time, I expect that different particles have almost the same persistence length.

Response (3): We thank the reviewer for this insightful observation. Although the translational speeds v_0 of the robots are comparable, the persistence length $l = v_0\tau_r$ is also determined by the persistence times $\tau_r = 1/D_r$, which is affected by the rotational diffusion. Our measurements show that τ_r varies among the different robots, resulting in distinct persistence lengths despite the nearly constant speed v_0. The extracted persistence lengths for all robots and the corresponding parameter-extraction procedures have been included in the revised manuscript.

Comment (4): In the introduction or conclusion, the authors should mention other realizations of active granular particles showing circular motion, i.e. chiral:
*** Vega Reyes, F., López-Castaño, M. A., & Rodríguez-Rivas, Á. (2022). Diffusive regimes in a two-dimensional chiral fluid. Communications Physics, 5(1), 256.**
*** Caprini, L., Abdoli, I., Marconi, U. M. B., & Löwen, H. (2025). Spontaneous self-wrapping in chiral active polymers. Newton 2025. DOI: 10.1016/j.newton.2025.100253.**

Response (4): We thank the reviewer for pointing out these relevant studies. The suggested references have been added to the Introduction of the revised manuscript.

Text changes:

1. Page 1, left column, first paragraph

It was: "CAPs are found across a wide range of systems and length scales, from nanoscale motor proteins [19], microscale sperm cells [20, 21] and interface-circling bacteria [22, 23], to chiral colloids [24, 25], starfish embryos [10], and centimeter-scale vibrated robots [26-33]."

New reads: "Chiral active particles are observed across a wide range of systems and length scales, from nanoscale motor proteins [19], microscale sperm cells [20, 21] and interface-circling bacteria [22, 23], to chiral colloids [24, 25], starfish embryos [10], centimeter-scale vibrated robots and rotors [26-33, Commun. Phys. 5, 256 (2022)], and chiral active polymers [Newton 1, 100253 (2025)]."

Comment (5): The theoretical result (Eq. (3)) was first derived in the following

paper:
*** Van Teeffelen, S., & Löwen, H. (2008). Dynamics of a Brownian circle swimmer. Physical Review E—Statistical, Nonlinear, and Soft Matter Physics, 78(2), 020101.**
The authors should also mention other papers where the theory of potential-free or confined chiral active particles has been considered:
*** Sevilla, F. J. (2016). Diffusion of active chiral particles. Physical Review E, 94(6), 062120.**
*** Caprini, L., & Marconi, U. M. B. (2019). Active chiral particles under confinement: Surface currents and bulk accumulation phenomena. Soft Matter, 15(12), 2627-2637.**
*** Joshi, J., & Mishra, S. (2025). Analytical Theory of Chiral Active Particle Transport in a Fluctuating Density Field. arXiv preprint arXiv: 2508.15366.ù**
*** Caprini, L., Löwen, H., & Marconi, U. M. B. (2023). Chiral active matter in external potentials. Soft Matter, 19(33), 6234-6246.**

Response (5): We thank the reviewer for pointing out the foundational work of Van Teeffelen & Löwen and the additional relevant studies. We have now cited these references appropriately and expanded the Introduction in the revised manuscript.

Text changes:

1. Page 5, right column, third paragraph

It was: "Theoretically, the effective diffusion coefficient of a CAP in obstacle-free space can be expressed as [53] ……"

New reads: "In the annular channel geometry, CABP motion along the azimuthal direction θ is effectively unconfined and experiences periodic boundary conditions. Consequently, the measured angular displacement $\Delta\theta$ can exceed 2π. Under obstacle-free conditions, the effective diffusion coefficient of a CABP can therefore be expressed theoretically as [Phys. Rev. E. 78, 020101 (2008), Phys. Rev. E. 94, 062120 (2016), 63] ……"

2. Page 1, right column, first paragraph

It was: "In free space, CAPs typically follow circular trajectories in two dimensions and helical paths in three dimensions [1]."

New reads: "In free space, CABPs typically follow circular trajectories in two dimensions and helical paths in three dimensions [1], while their chirality further modulates orientational persistence and can generate oscillatory kurtosis under strong torque conditions [Phys. Rev. E. 94, 062120 (2016)]."

3. Page 1, right column, first paragraph

It was: "In such contexts, CAPs transport behaviors can deviate significantly from that in homogeneous systems [39-42], such as directional locking [3] and spin-dependent segregation [43, 44]."

New reads: "In such contexts, CABPs transport can deviate significantly from that in homogeneous systems [42-45], exhibiting phenomena such as directional locking [3], spin-dependent segregation [46, 47], chirality-induced steady momentum currents and bulk accumulation [Soft Matter 15, 2627 (2019)], deviations from Maxwell–Boltzmann behavior that vanish when chirality or radial symmetry is absent [Soft Matter 19, 6234 (2023)], and chirality–density coupling that renormalizes orientational persistence and generates nontrivial dynamical crossovers [arXiv:2508.15366 (2025)]."

Comment (6): The non-monotonic dependence of the diffusion coefficient with density has already been observed in numerical simulations, for instance, in
*** Van Roon, D. M., Volpe, G., da Gama, M. M. T., & Araújo, N. A. (2022). The role of disorder in the motion of chiral active particles in the presence of obstacles. Soft Matter, 18(36), 6899-6906.**
The authors should comment on this.

Response (6): We thank the reviewer for this important suggestion. We have added a discussion of the findings by van Roon *et al.* [Soft Matter 18, 6899, (2022)] in the updated manuscript, emphasizing the consistency between their reported non-monotonic diffusion behavior and our experimental observations.

Text changes:

1. Page 1, right column, first paragraph

It was: "Notably, CAPs exhibit pronounced diffusion enhancement in disordered obstacles [4, 45–47], in stark contrast to the diffusion suppression typically observed for linear self-propelled particles under analogous conditions [48–51]. These findings underscore the role of chirality in governing particle-environment interactions and indicate that obstacle disorder, noise, and density act as tunable parameters for regulating active transport.”

New reads: “Notably, CABPs exhibit pronounced diffusion enhancement in disordered obstacles [4, 51–53], a similar counterintuitive enhancement has recently been observed for self-propelled polymer-like worms in disordered media [Phys. Rev. Lett. 134, 128303 (2025)], in stark contrast to the diffusion suppression typically observed for linear self-propelled particles under analogous conditions [55–58]. Numerical simulations by van Roon *et al.* further indicate that the diffusivity of CABPs depends nonmonotonically on obstacle density, arising from the interplay between chirality and static disorder that induces orbit rectification and channeling [Soft Matter 18, 6899 (2022)]. This characteristic nonmonotonic response, rooted in the redirection of intrinsic self-propulsion, represents a transport mechanism specific to CABPs and is absent in pure rotors lacking self-propulsion [Europhys. Lett. 92, 64004 (2010)]. Collectively, these results underscore the role of chirality in particle-environment interactions and indicate that obstacle disorder, noise, and density act as tunable parameters for active transport.”

Comment (7): In the theoretical prediction (3), the authors state that τ_r is the rotational relaxation time given by the rotational friction coefficient γ_r and the temperature T. This is not correct. Indeed, τ_r is the particle persistence time, which for a single particle is an intrinsic parameter of the dynamics. This time is often identified as the autocorrelation time of the orientation or through the mean-square displacement, specifically as the time needed to approach a diffusive behavior from the ballistic behavior induced by the activity. In addition, the authors should clarify the equalities, $\gamma_r = t_m/t_{tot}$ and $\gamma_t = v_0/v$, adding more details and explaining why this is true.

Response (7): We thank the reviewer for this important clarification. For a single active particle, the persistence time (i.e., the rotational relaxation time) τ_r is indeed an intrinsic dynamical parameter, commonly defined through the orientational autocorrelation function or equivalently as the timescale governing the crossover from ballistic to diffusive motion.

In our framework, τ_r is treated as an effective persistence time associated with the particle’s rotational dynamics and written as $\tau_r = 1/D_r = \frac{\gamma_r}{k_B T}$, where D_r is the effective rotational diffusion coefficient and γ_r is an effective rotational friction [Phys. Rev. E. 78, 020101 (2008), 63]. In the presence of obstacles, particle–environment collisions renormalize both rotational and translational dynamics. While substrate friction can be regarded as constant, additional effective friction from collisions with soft rings depends on the obstacle area fraction ϕ. To quantify this effect, we introduce empirical relations $\gamma_{\mathrm{r}}(\phi) \propto t_{\mathrm{m}}/t_{\mathrm{tot}}$ and $\gamma_t(\phi) \propto v_0/v$, linking effective friction coefficients to experimentally measurable observables. Increasing obstacle density suppresses reorientation events, making it more difficult for the particle to alter its direction of motion, and enhances directional persistence, reflected by the increase of $t_{\mathrm{m}}/t_{\mathrm{tot}}$ and interpreted as an increase in effective rotational friction $\gamma_{\mathrm{r}}(\phi)$. Similarly, the reduction of the migration speed v reflects the enhancement of translational friction, $\gamma_t(\phi) \propto v_0/v$.

These relations are effective scaling descriptions capturing how obstacle-induced collimation and velocity suppression renormalize particle dynamics. The definition of τ_r and the physical meaning of $\gamma_{\mathrm{r}}(\phi)$ and $\gamma_t(\phi)$ have been clarified in the revised manuscript.

Text change:

Page 5, right column, third paragraph

It was: "Theoretically, the effective diffusion coefficient of a CAP in obstacle-free space can be expressed as [53] …… Here, Eq. (3) remains applicable ...... The relations are given by $\gamma_r(\phi) \propto t_{\mathrm{m}}/t_{\mathrm{tot}}$ and $\gamma_t(\phi) \propto v_0/v$."

New reads: "In the annular channel geometry, CABP motion along the azimuthal direction θ is effectively unconfined and experiences periodic boundary conditions. Consequently, the measured angular displacement $\Delta\theta$ can exceed 2π. Under obstacle-free conditions, the effective diffusion coefficient of a CABP can therefore be expressed theoretically as [Phys. Rev. E. 78, 020101 (2008), Phys. Rev. E. 94, 062120 (2016), 63],

$$D = D_t^T + \frac{v^2\tau_r}{2[1+(\omega\tau_r)^2]}. \tag{3}$$

For a CABP moving in obstacle-free space, the thermal translational diffusion coefficient is given by $D_t^T = k_B T/\gamma_t^0$. The rotational relaxation time (i.e., the persistence time) is defined as $\tau_r = 1/D_r = \gamma_r^0/(k_B T)$, where D_r is the rotational diffusion coefficient extracted from the mean-squared angular displacement (MSAD) or orientation autocorrelation [Soft Matter 12, 4584 (2016), J. Chem. Phys. 121, 11322 (2004)]. The translational and angular velocity are $v_0 = F_d/\gamma_t^0$ and $\omega_0 = T_d/\gamma_r^0$, respectively, with γ_t^0 and γ_r^0 being the translational and rotational friction coefficients in obstacle-free space, and F_d and T_d the driving force and torque acting on the particle.

Accordingly, the effective diffusion coefficients in obstacle-free space can be approximated as

$$D_0 = k_B T/\gamma_t^0 + \frac{{F_d}^2 \gamma_r^0/{\gamma_t^0}^2}{2k_B T\left[1+(\frac{T_d}{k_B T})^2\right]} \tag{4}$$

The environment with increasing obstacle area fraction ϕ simultaneously modifies translational and rotational dynamics. Frequent collisions suppress the migration speed, thereby enhancing the effective translational friction $\gamma_t(\phi)$, while the obstacle-induced alignment enhances orientational persistence, effectively reducing the rotational diffusion coefficient and leading to an increased effective rotational friction $\gamma_r(\phi)$. These effects motivate us to treat both friction coefficients as ϕ-dependent. Experimentally, they are captured by the empirical relations $\gamma_r(\phi) \propto t_{\mathrm{m}}/t_{\mathrm{tot}}$ and $\gamma_t(\phi) \propto v_0/v$, which quantify the enhancement of directional persistence and the suppression of migration speed, respectively. By substituting these relations into Eq. (4) yields the generalized diffusion coefficient in obstacle-rich environments,

$$D = k_B T/\gamma_t(\phi) + \frac{{F_d}^2 \gamma_r(\phi)/\gamma_t(\phi)^2}{2k_B T\left[1+(\frac{T_d}{k_B T})^2\right]}. \tag{5}$$

Since the thermal translational term $D_t^T = k_B T/\gamma_t(\phi)$ is negligibly compared with the activity-induced contribution, the effective diffusion coefficients of particles in the presence and absence of obstacles can be approximated as

$$D \approx \frac{{F_d}^2 \gamma_r(\phi)/\gamma_t(\phi)^2}{2k_B T\left[1+(\frac{T_d}{k_B T})^2\right]}, \tag{6}$$

$$D_0 \approx \frac{{F_d}^2 \gamma_r^0/{\gamma_t^0}^2}{2k_B T\left[1+(\frac{T_d}{k_B T})^2\right]}. \tag{7}$$

Consequently, the normalized diffusion coefficient becomes

$$\frac{D}{D_0} = \frac{\gamma_r(\phi){\gamma_t^0}^2}{\gamma_t^2(\phi)\gamma_r^0}. \qquad (8)\text{”}$$

Comment (8): In this paper, theoretical predictions are not derived. The authors should specify that they have developed a scaling argument.

Response (8): We thank the reviewer for this clarification. Our analysis is based on a self-consistent scaling argument rather than on a full theoretical derivation. Referring to it as a “theoretical prediction” without qualification may be misleading. In the revised manuscript, we have explicitly referred to our approach as a scaling argument and clarified that it is intended to rationalize the observed nonmonotonic diffusion by linking the macroscopic transport behavior to independently measured microscopic dynamical quantities.

Text change:

Page 6, right column, first paragraph

It was: "These results demonstrate that the theoretical predictions capture the essential physics underlying the experimentally observed nonmonotonic diffusion of CAPs in complex media."

New reads: "These results demonstrate that the empirical functions together with the scaling arguments capture the essential physics underlying the experimentally observed nonmonotonic diffusion of CABPs in complex media."

Comment (9): The authors report some empirical functions that capture the behavior of the functions γ_r and γ_t. The authors should remove this fitting analysis: there is no point in these predictions, which are not supported by theory and therefore do not add anything to the present paper.

Response (9): We thank the reviewer for raising this important point. The empirical fitting functions for γ_r and γ_t are not intended to represent theoretical predictions, and we have explicitly clarified that these functions are empirical and not theoretically derived in the revised manuscript. Nevertheless, the empirical analysis is retained because it provides a quantitative connection between experimentally measured dynamical observables and the proposed scaling argument. The fitted forms of γ_r and γ_t enable us to assess whether the scaling framework can consistently account for the observed nonmonotonic diffusion of CABPs in obstacle environments. Their role is therefore limited to a quantitative consistency check rather than a predictive theoretical model.

Text change:

1. Page 6, left column, the last paragraph

It was: "On this basis, the theoretical prediction from Eq. (6), ……"

New reads: "On this basis, the empirical prediction from Eq. (8), ……"

2. Page 6, right column, first paragraph

It was: “These results demonstrate that the theoretical predictions capture the essential physics underlying the experimentally observed nonmonotonic diffusion of CAPs in complex media.”

New reads: “These results demonstrate that the empirical functions together with the scaling arguments capture the essential physics underlying the experimentally observed nonmonotonic diffusion of CABPs in complex media.”

Minor points:
- page 1 “hyperuniform” --> “hyperuniformity”
- page 1. “In this Letter” --> “In this paper”

Text change:

1. Page 1, left column, first paragraph

It was: “……, resulting in rich unconventional phenomena, including odd viscosity [5–8], odd elasticity [9–11], hyperuniform [12, 13] ......”

New reads: “…… resulting in rich unconventional phenomena, including odd viscosity [5–8], odd elasticity [9–11], hyperuniformity [12, 13] ......”

2. Page 2, left column, third paragraph

It was: “In this Letter, ...”

New reads: “In this paper, …...”

Response to the comments from Reviewer 2

General comment:

This manuscript studies the motion of a CAP in a system of deformable and displaceable obstacles on a vibrating stage. This work serves as a valuable complement to previous studies on particle motion in rigid and fixed obstacle arrays. It is known that particle motion can be suppressed by obstacles and promoted by 1D-like channels between obstacles, leading to a non-monotonic dependence of particle diffusion on obstacle density. The authors successfully reproduce this expected behavior and further demonstrate that diffusion at certain intermediate obstacle densities can be up to 100 times higher than in the obstacle-free case. While the findings are interesting, the authors should address the following major points before I can recommend publication:

Response: We sincerely thank the reviewer for the positive evaluation and recognition of our work. We have carefully revised the manuscript, supplemented additional analyses where appropriate, and addressed all comments point by point below.

Comment (1): The function q(θ) in Eq. (2) contains an arbitrarily defined parameter b. Why not replace Q(t) with a standard autocorrelation function of the particle's orientation, which would be unambiguous with a clear meaning?

Response (1): The standard orientation autocorrelation function of chiral active Brownian particles (CABPs) orientation, $C_\theta(\mathrm{t})=\langle \vec{e}(t_0)\cdot\vec{e}(t+t_0)\rangle = e^{-t/\tau_r}$, provides an unambiguous characterization of rotational dynamics, with the decorrelation time τ_r related to the rotational diffusion coefficient by $\tau_r = 1/D_r$ in two dimensions [Eur. Phys. J. E 40, 23 (2017)]. For completeness, the corresponding of τ_r and D_r in obstacle-free space are reported in Table 1 of the revised manuscript.

The primary focus of this work, however, is not to quantify the rotational diffusion, but to identify dynamical heterogeneity in obstacle environments, where CABPs motion alternates between trapped and migratory states. For this purpose, the self-part of the two-point overlap correlation function $Q(\mathrm{t})$ is employed, as commonly used to probe local confinement and cage effects in heterogeneous dynamics [Nat. Commun. 11, 2581 (2020), Proc. Natl. Acad. Sci. USA 116, 22977 (2019)]. The parameter b sets a characteristic angular scale for confinement and the qualitative behavior of $Q(\mathrm{t})$ is robust to reasonable variations of b [Supplementary Material]. Thus, while $C_{\theta}(t)$ characterizes rotational decorrelation of CABP, Q(t) is better suited for resolving local trapping and dynamical heterogeneity, which is the central objective of this study. To improve clarity, the Results section of the revised manuscript has been reorganized into distinct subsections.

Text changes:

1. Page 2, Fig. 1

It was:

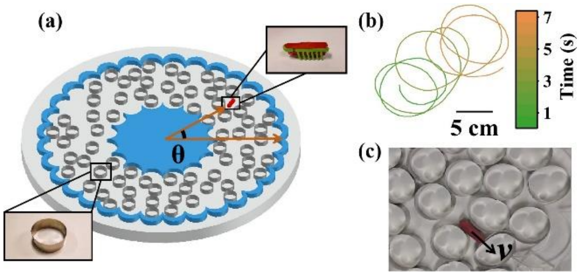

(b) Time-colored trajectory of a CAP with r = 4.46 cm in free space. (c) Deformation of soft rings under compressive stress exerted by CAP motion. Black arrow indicates the direction of motion.

New reads:

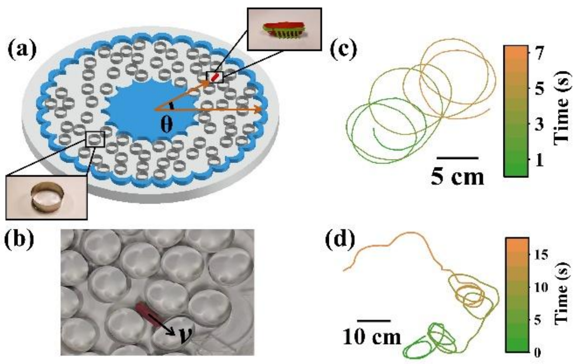

(b) Deformation of soft rings under compressive stress exerted by CABP motion. Black arrow indicates the direction of motion. Time-colored trajectory of a CAP with r = 4.46 cm in the (c) absence of obstacles and (d) presence of obstacles at ϕ = 0.50.

2. Page 4, right column, first paragraph

It was: "This heterogeneity arises from the coexistence of two dominant motility modes, namely a slow, localized trapped state and a fast, persistent migration state."

New reads: "This heterogeneity arises from the coexistence of two dominant motility modes, namely a slow, localized trapped state and a fast, persistent migration state, as exemplified by CABP motion in the presence of obstacles at ϕ=0.50 [Fig. 1(d)]."

Comment (2): The specific criterion used to identify "trapped" and "migration" states should be explicitly defined and provided in the manuscript.

Response (2): We thank the reviewer for this helpful suggestion. A particle is classified as trapped if it remains confined within a circular region of radius R_c centered at its initial position and completes at least two full rotations. The confinement radius R_c is determined from the characteristic confinement length at a given obstacle area fraction ϕ and is defined as the average diameter of all identified trapped regions [Supplementary Material]. If the residence time within the R_c region is shorter than two rotational periods, the CABP is classified as migratory. In the revised manuscript, we have explicitly defined the criterion used to distinguish trapped and migration states.

Text changes:

Page 3, right column, first paragraph

It was: "The CAP is defined as being in the trapped state if it remains within a radius R_c from its initial position and completes at least two rotations, with R_c determined from the characteristic confinement scale at a given ϕ."

New reads: "The CABP is defined as being in the trapped state if it remains within a circular region of radius R_c centered at its initial position and completes at least two rotations. The confinement radius R_c is determined by the characteristic confinement scale at a given obstacle area fraction ϕ and is defined as the average diameter of all identified trapped regions [the details in the Supplementary Material]. Otherwise, if the residence time within the R_c region is shorter than two rotational periods, the CABP is classified as being in the migration state."

Comment (3): The rationale behind the metric $v^2 t_m/(v_0^2 t_{tot})$ needs to be explained. Please clarify why this specific combination is chosen to capture the combined effects.

Response (3): We thank the reviewer for this helpful comment. The metric $v^2 t_m/(v_0^2 t_{tot})$ is introduced as a physically motivated and dimensionless measure that captures the combined effects of obstacle-induced changes in migration speed and directional persistence.

As the obstacle area fraction increase, frequent particle–obstacle collisions produce two coupled effects. The translational motion is suppressed, leading to a reduction in the migration speed v, and random reorientation events are hindered, making changes in the direction of motion less frequent. The latter effect enhances directional persistence, which is quantified by the increase in the migration time t_m. The product $v^2 t_m$ therefore naturally captures the concurrent reduction in speed and enhancement of persistence. In addition, $v^2 t_m$ has the same physical dimension as a diffusion coefficient. Normalizing this quantity by its counterpart in obstacle-free space, $v_0^2 t_{tot}$, extracts the influence of the obstacle background and yields a dimensionless characterization of the modified transport properties.

To further demonstrate the robustness of this interpretation, we have also analyzed the quantity $vt_m/(v_0 t_{tot})$ as a function of the obstacle area fraction ϕ [Fig. R2], which exhibits the same nonmonotonic behavior and the same optimal obstacle fraction ϕ_c as $v^2 t_m/(v_0^2 t_{tot})$. This confirms that the nonmonotonicity originates from the competition between obstacle-induced the enhancement of CABPs motion collimation and the suppression of their migration velocity. Corresponding clarifications have been added to the revised manuscript.

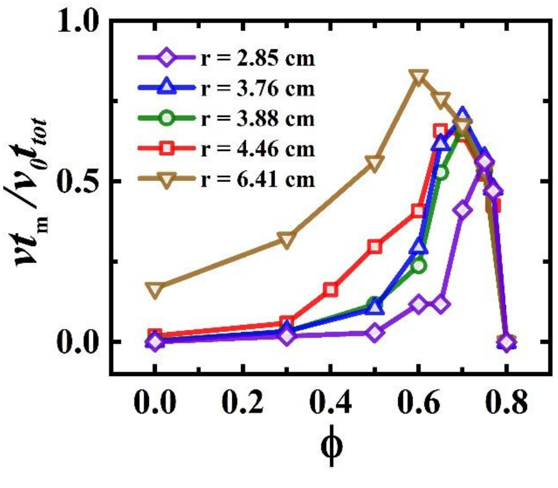

Fig. R2. The relations between $vt_m/(v_0 t_{tot})$ of different CABPs and obstacle area fraction ϕ.

Text changes:

Page 5, right column, second paragraph

It was: "To validate the competing mechanisms underlying CAP diffusion, we evaluate the ratio $v^2 t_m / v_0^2 t_{tot}$, which captures the combined effects of obstacles on the motion collimation and velocity suppression."

New reads: "To validate the competing mechanisms underlying CABP diffusion, we evaluate the ratio $v^2 t_m / (v_0^2 t_{tot})$, which captures the combined effects of obstacle-induced motion collimation and velocity suppression. As the obstacle area fraction increases, CABP–obstacle collisions reduce the migration speed v while simultaneously enhancing directional persistence, as reflected by an increase in t_m. Because the product $v^2 t_m$ has the same physical dimension as the diffusion coefficient, the normalized ratio provides a natural, dimensionless measure of the effective diffusion behavior."

Comment (4): The origin and derivation of Eqs. (4) and (5) should be stated. Please provide a reference or derivation.

Response (4): We thank the reviewer for this helpful suggestion. In the revised manuscript, we have added a detail derivation of Eqs. (4) and (5) clarify their physical origin.

Text changes:

Page 5, right column, third paragraph

It was: "Theoretically, the effective diffusion coefficient of a CAP in obstacle-free space can be expressed as [53] …… The relations are given by $\gamma_r(\phi) \propto t_{\mathrm{m}}/t_{\mathrm{tot}}$ and $\gamma_t(\phi) \propto v_0/v$."

New reads: "In the annular channel geometry, CABP motion along the azimuthal direction θ is effectively unconfined and experiences periodic boundary conditions. Consequently, the measured angular displacement $\Delta\theta$ can exceed 2π. Under obstacle-free conditions, the effective diffusion coefficient of a CABP can therefore be expressed theoretically as [Phys. Rev. E. 78, 020101 (2008), Phys. Rev. E. 94, 062120 (2016), 63],

$$D = D_t^T + \frac{v^2 \tau_r}{2[1 + (\omega \tau_r)^2]} \tag{3}$$

For a CABP moving in obstacle-free space, the thermal translational diffusion coefficient is given by $D_t^T = k_B T / \gamma_t^0$. The rotational relaxation time (i.e., the persistence time) is defined as $\tau_r = 1/D_r = \gamma_r^0/(k_B T)$, where D_r is the rotational diffusion coefficient extracted from the mean-squared angular displacement (MSAD) or orientation autocorrelation [Soft Matter 12, 4584 (2016), J. Chem. Phys. 121, 11322 (2004)]. The translational and angular velocity are $v_0 = F_d/\gamma_t^0$ and $\omega_0 = T_d/\gamma_r^0$, respectively, with γ_t^0 and γ_r^0 being the translational and rotational friction coefficients in obstacle-free space, and F_d and T_d the driving force and torque acting on the particle.

Accordingly, the effective diffusion coefficients in obstacle-free space can be approximated as

$$D_0 = k_B T/\gamma_t^0 + \frac{{F_d}^2\gamma_r^0/{\gamma_t^0}^2}{2k_B T\left[1+(\frac{T_d}{k_B T})^2\right]} \tag{4}$$

The environment with increasing obstacle area fraction ϕ simultaneously modifies translational and rotational dynamics. Frequent collisions suppress the migration speed, thereby enhancing the effective translational friction $\gamma_t(\phi)$, while the obstacle-induced alignment enhances orientational persistence, effectively reducing the rotational diffusion coefficient and leading to an increased effective rotational friction $\gamma_r(\phi)$. These effects motivate us to treat both friction coefficients as ϕ-dependent. Experimentally, they are captured by the empirical relations $\gamma_r(\phi) \propto t_{\mathrm{m}}/t_{\mathrm{tot}}$ and $\gamma_t(\phi) \propto v_0/v$, which quantify the enhancement of directional persistence and the suppression of migration speed, respectively. By substituting these relations into Eq. (4) yields the generalized diffusion coefficient in obstacle-rich environments,

$$D = k_B T/\gamma_t(\phi) + \frac{{F_d}^2\gamma_r(\phi)/\gamma_t(\phi)^2}{2k_B T\left[1+(\frac{T_d}{k_B T})^2\right]}. \tag{5}$$

Since the thermal translational term $D_t^T = k_B T/\gamma_t(\phi)$ is negligibly compared with the activity-induced contribution, the effective diffusion coefficients of particles in the presence and absence of obstacles can be approximated as

$$D \approx \frac{{F_d}^2\gamma_r(\phi)/\gamma_t(\phi)^2}{2k_B T\left[1+(\frac{T_d}{k_B T})^2\right]}, \tag{6}$$

$$D_0 \approx \frac{{F_d}^2\gamma_r^0/{\gamma_t^0}^2}{2k_B T\left[1+(\frac{T_d}{k_B T})^2\right]}. \tag{7}$$

Consequently, the normalized diffusion coefficient becomes

$$\frac{D}{D_0} = \frac{\gamma_r(\phi){\gamma_t^0}^2}{\gamma_t^2(\phi)\gamma_r^0}. \tag{8}$$”

Comment (5): The term “deformable” is highlighted in the title, abstract, and discussion, but the degree of deformability is not quantified. A rough estimate of the obstacle deformation under the given particle activity is needed. Furthermore,

some obstacles in the videos appear non-circular. Could particle collisions induce irreversible (plastic) deformation? The potential effects of both deformation and non-circular shape should be discussed.

Response (5): We thank the reviewer for these insightful suggestions. To quantify the obstacle deformation, we analyzed the obstacle shapes and evaluated their circularity, defined as $C = 4\pi S_r/L_P^2$, where S_r and L_P denote the area enclosed by a ring and its perimeter, respectively. For a perfect circle, $C = 1.0$. As shown in Fig. R3, the average circularity of the soft rings remains $C > 0.8$ across all obstacle area fractions ϕ explored in the experiments in the presence of active particle motion, indicating that the soft rings remain largely circular and that deformations under the present conditions are small and elastic.

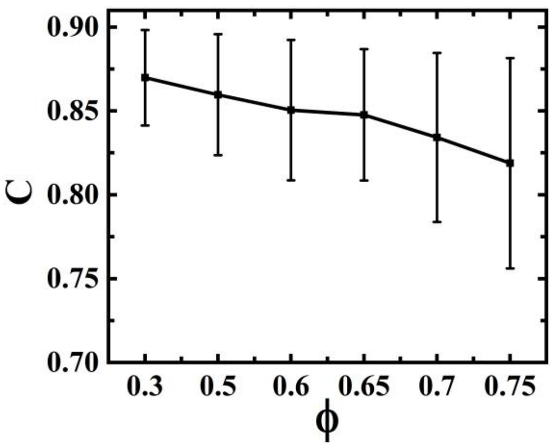

Fig. R3. Circularity $C = 4\pi S_r/{L_P}^2$ of the soft rings at different obstacle area fractions ϕ in the presence of a CABP with *r*=3.76 cm.

The apparent non-circular shapes observed in the videos arise primarily from experimental and imaging factors rather than irreversible deformation. In particular, the imaging geometry, with the camera positioned above the center of the annular setup, may introduce slight visual distortions and shadow effects near the ring boundaries. In addition, transparent tape used at the attachment points of the soft rings can locally reduce curvature, leading to small deviations from perfect circularity. These features are inherent to the experimental setup and consistent across experiments.

Finally, these minor geometric imperfections and slight elastic deformations in our system do not qualitatively affect the physical mechanisms discussed. We note that stronger deformations, such as leading to rod-like or highly elongated obstacles, could potentially alter the transport behavior and merit future investigation. A quantitative analysis of obstacle deformability and corresponding clarifications have been added to the revised manuscript and the Supplementary Material.

Text changes:

1. Page 3, right column, first paragraph

At the end of the first paragraph, we added the following sentences: "The non-circular shapes observed in the videos mainly arise from experimental and imaging factors rather than irreversible deformation. In particular, local curvature variations result from the tape used to fix the soft rings, while the imaging geometry introduces slight distortions near the ring boundaries. The small elastic deformations of the rings were quantified at different obstacle area fractions ϕ in the presence of a CABP with r=3.76 cm [Supplementary Material]. We speculate that substantially stronger deformations, such as leading to rod-like or highly elongated obstacles, may potentially modify the transport behavior and warrant future investigation."

Comment (6): Are the two videos under the same obstacle density? Captions for both videos are missing.

Response (6): We thank the reviewer for this helpful suggestion. The two videos correspond to different obstacle area fractions, showing the motion of a representative CABP with r=3.88 cm at $\phi = 0.60$ (trapped state) and $\phi = 0.70$ (migrating state), respectively. Clear captions specifying the obstacle densities have been added to the Supplementary Videos and the manuscript has been updated accordingly.

Text changes:

1. Page 3, right column, first paragraph

It was: "Within these regions, CAPs exhibit confined circular motion, resulting in markedly suppressed diffusion [see the movies in the Supplementary Material]."

New reads: "Within these regions, CABPs exhibit confined circular motion, resulting in markedly suppressed diffusion, as exemplified by a CABP with an orbital radius of 3.88 cm at an obstacle area fraction of 0.60 [see the movies in the Supplementary Material]."

2. Page 3, right column, first paragraph

It was: “In the migrating state, CAPs undergo successive inelastic collisions with surrounding deformable rings, which gradually reorient their motion and support sustained quasi-linear trajectories [see the movies in the Supplementary Material].”

New reads: “In the migrating state, CABPs undergo successive inelastic collisions with surrounding deformable rings, which gradually reorient their motion and support sustained quasi-linear trajectories, as illustrated by a particle with an orbital radius of 3.88 cm at $\phi = 0.70$ [see the movies in the Supplementary Material].”

Minor Comments:

1. Given the relatively small system size, are boundary effects pronounced? It would be straightforward to study a larger system to confirm the results are not influenced by finite-size effects.

Response (1): We thank the reviewer for raising this important point. Although the system size is relatively small, boundary effects do not significantly influence the transport behavior reported here. Both the inner and outer boundaries are composed of petal-shaped arc segments, which effectively suppress persistent staying at the boundaries and thus minimize boundary-dominated transport [Nat. Commun. 5, 4688 (2014)]. Moreover, our analysis focuses on one-dimensional angular diffusion along the azimuthal direction θ. In this annular geometry, radial motion is confined, while diffusion in θ effectively experiences periodic boundary conditions. Provided that R_{out} is much larger than the particle orbital radius r, variations in the radial boundaries do not qualitatively affect the observed nonmonotonic diffusion. In addition, the present system is strongly dissipative and overdamped, so the finite-size effects in the periodic azimuthal direction, that arises from the long-distance momentum transfer, is negligible, unlike momentum-conserved hydrodynamic systems.

To further support this conclusion, we performed control experiments with varying obstacle size, softness, and confinement geometry, all of which consistently exhibit the same nonmonotonic diffusion behavior, confirming that the results are not influenced by finite-size or boundary effects [Supplementary Material].

Text changes:

1. Page 5, right column, third paragraph

It was: “Theoretically, the effective diffusion coefficient of a CAP in obstacle-free space can be expressed as [53] ……”

New reads: “In the annular channel geometry, CABP motion along the azimuthal direction θ is effectively unconfined and experiences periodic boundary conditions. Consequently, the measured angular displacement $\Delta\theta$ can exceed 2π. Under obstacle-free conditions, the effective diffusion coefficient of a CABP can therefore be expressed theoretically as [Phys. Rev. E. 78, 020101 (2008), Phys. Rev. E. 94, 062120 (2016), 63] ……”

2. Page 3, left column, first paragraph

At the end of the first paragraph, we added the following sentences: “Additional control experiments varying obstacle size, softness, and confinement geometry consistently confirm the robustness of this nonmonotonic diffusion behavior [Supplementary Material].”

2. Please clarify if the measured angular displacement $\Delta\theta$ can exceed 2π.

Response (2): We thank the reviewer for this helpful clarification suggestion. The measured angular displacement $\Delta\theta$ can indeed exceed 2π. In the annular channel geometry, CABP motion along the azimuthal direction θ is effectively unconfined and experiences periodic boundary conditions. Consequently, $\Delta\theta$ is not restricted to the interval $[0, 2\pi]$ and can increase beyond 2π over time.

Text changes:

1. Page 5, right column, third paragraph

It was: “Theoretically, the effective diffusion coefficient of a CAP in obstacle-free space can be expressed as [53] ……”

New reads: “In the annular channel geometry, CABP motion along the azimuthal direction θ is effectively unconfined and experiences periodic boundary conditions. Consequently, the measured angular displacement $\Delta\theta$ can exceed 2π. Under obstacle-free conditions, the effective diffusion coefficient of a CABP can therefore be expressed theoretically as [Phys. Rev. E. 78, 020101 (2008), Phys. Rev. E. 94, 062120 (2016), 63] ……”

Response to the comments from Reviewer 3

General comment:

The motion of self-propelled particles interacting with soft obstacles is investigated in annular confinement conditions. The experimental part of the study is performed with commercial Hexbugs whose legs are modified to perform helical motions with variable orbital radius. Results are compared with an analytical description partly developed for dense active matter systems and here adapted with an empirical estimation of the relevant functions. The transition between trapping and migrating has been recently described for active polymerlike worms interacting with and movable obstacles (PRL 134, 128303 (2025), arXiv:2503.15755). In spite the differences, it seems that the transition between trapping and migrating is a common property of both systems. In the title and the overall manuscript, the system under study is described as a paradigm of chiral active particles. Meanwhile, it is not so clear to me that the chirality of the particles plays a relevant role in the actual mechanism here described.

I like this work, and I am certain that a modified version of this manuscript deserves publication, but I am not sure about its suitability for Communication Physics.

I have various other comments that the authors might want to consider:

Response: We sincerely thank the reviewer for the positive assessment of our work. We have carefully revised the manuscript, supplemented additional analyses where appropriate, and addressed all comments point by point below.

Comment (1): In the introduction, no distinction is made between chiral active Brownian particles and rotors. CAPs are then referred as having both self-propulsion and autonomous rotation, which applies to their system but not to rotors. The authors could explain if this crucial conceptual difference has an effect in the observations they made.

Response (1): We thank the reviewer for pointing out this important conceptual distinction. Chiral active Brownian particles (CABPs) and rotors differ fundamentally in their dynamics. CABPs combine persistent self-propulsion with autonomous rotation, whereas ideal rotors undergo torque-driven rotation without self-propulsion. Consequently, an isolated ideal rotor remains spatially localized and does not exhibit long-range translational diffusion with translation arises only from many-body collision or hydrodynamic interactions [Europhys. Lett. 92, 64004 (2010)]. In contrast, an isolated CABP already displays persistent translational motion with chirality shaping its trajectory.

The diffusion enhancement reported in this work relies critically on this intrinsic self-propulsion. Interactions with obstacles can redirect and collimate the propulsive motion of CABPs, giving rise to a migrating state with enhanced directional persistence and long-range transport. Such a mechanism is absent for pure rotors. Although obstacle-induced collisions may generate weak, fluctuation-driven translational motion for rotors, these effects are qualitatively distinct and are not expected to produce the pronounced, nonmonotonic diffusion enhancement observed in our system. This distinction between CABPs and rotors has been explicitly clarified in the revised introduction.

Text changes:

1. Page 1, Abstract

It was: "Chiral active particles (CAPs), which intrinsically break both time-reversal and parity symmetries, drive systems far from equilibrium and exhibit rich nonequilibrium dynamics."

New reads: "Chiral active Brownian particles (CABPs) convert stored or environmental energy into both self-propulsion and autonomous rotation, intrinsically breaking time-reversal and parity symmetries, driving systems far from equilibrium, and exhibiting rich nonequilibrium dynamics."

2. Page 1, left column, first paragraph

It was: "Chiral active particles (CAPs) represent a unique class of active matter capable of converting internal or environmental energy into both self-propulsion and autonomous rotation, thereby simultaneously breaking time-reversal and parity symmetries. This intrinsic symmetry breaking drives systems far from equilibrium, resulting in rich unconventional phenomena, including odd viscosity [5–8], odd elasticity [9–11], hyperuniform [12, 13] ......"

New reads: "Chiral active particles represent a unique class of active matter capable of converting internal or environmental energy into autonomous rotation, thereby driving systems far from equilibrium and resulting in rich unconventional phenomena, including odd viscosity [5–8], odd elasticity [9–11], hyperuniformity [12, 13] ......"

3. Page 1, left column, first paragraph

It was: "CAPs are found across a wide range of systems and length scales, from nanoscale motor proteins [19], microscale sperm cells [20, 21] and interface-circling bacteria [22, 23], to chiral colloids [24, 25], starfish embryos [10], and centimeter-scale vibrated robots [26-33]. Their ubiquity and characteristic dynamics make them a powerful model for probing the fundamental principles of nonequilibrium statistical mechanics and active matter physics."

New reads: "Chiral active particles are observed across a wide range of systems and length scales, from nanoscale motor proteins [19], microscale sperm cells [20, 21] and interface-circling bacteria [22, 23], to chiral colloids [24, 25], starfish embryos [10], centimeter-scale vibrated robots and rotors [26-33, Commun. Phys. 5, 256 (2022)], and chiral active polymers [Newton 1, 100253 (2025)]. In particular, Chiral active Brownian particles (CABPs) combine self-propulsion with autonomous rotation, proving a ubiquitous and powerful model for probing the fundamental principles of nonequilibrium statistical mechanics and active matter physics."

4. Page 1, right column, first paragraph

It was: "Notably, CAPs exhibit pronounced diffusion enhancement in disordered obstacles [4, 45–47], in stark contrast to the diffusion suppression typically observed for linear self-propelled particles under analogous conditions [48–51]. These findings underscore the role of chirality in governing particle-environment interactions and indicate that obstacle disorder, noise, and density act as tunable parameters for regulating active transport."

New reads: "Notably, CABPs exhibit pronounced diffusion enhancement in disordered obstacles [4, 51–53], a similar counterintuitive enhancement has recently been observed for self-propelled polymer-like worms in disordered media [Phys. Rev. Lett. 134, 128303 (2025)], in stark contrast to the diffusion suppression typically observed for linear self-propelled particles under analogous conditions [55–58]. Numerical simulations by van Roon *et al.* further indicate that the diffusivity of CABPs depends nonmonotonically on obstacle density, arising from the interplay between chirality and static disorder that induces orbit rectification and channeling [Soft Matter 18, 6899 (2022)]. This characteristic nonmonotonic response, rooted in the redirection of intrinsic self-propulsion, represents a transport mechanism specific to CABPs and is absent in pure rotors lacking self-propulsion [Europhys. Lett. 92, 64004 (2010)]. Collectively, these results underscore the role of chirality in particle-environment interactions and indicate that obstacle disorder, noise, and density act as tunable parameters for active transport."

5. Replace other occurrences of Chiral active particles, CAPs, and CAP with Chiral active Brownian particles, CABPs, and CABP, respectively.

Comment (2): In my opinion, since Figures 6b and 7a,c refer to the reference motion, it would be clearer if discussed much earlier, maybe directly after Fig 2 or even before.

Response (2): We thank the reviewer for this constructive suggestion. In the updated manuscript, the data originally shown in Fig. 6(b) have been moved to immediately follow Fig. 2(b) and are now presented as Fig. 2(c).

By contrast, Figs. 7(a) and 7(c) display representative free-space trajectories that are intended to be directly compared with Figs. 7(b) and 7(d), which show the corresponding trajectories in the presence of obstacles. Keeping these panels together enables a clear side-by-side comparison of how obstacles modify particle motion and supports the interpretation of the nonmonotonic dependence of the D/D_0 peak on the orbital radius. For this reason, the original placement of Figs. 7(a) and 7(c) has been retained. We believe that this partial reorganization improves the overall clarity and logical structure of the revised manuscript while preserving the physical comparisons central to our conclusion.

Text changes:

1. Page 3, Fig. 2

It was:

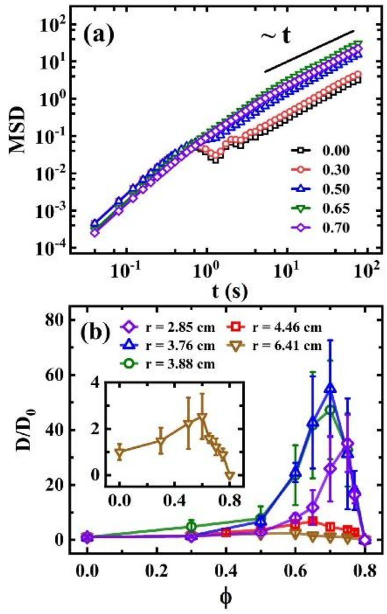

FIG. 2. (a) The MSD of a CAP with $r = 4.46$ cm as a function of delay time t at different ϕ. (b) The relation between ϕ and D/D_0 for CAPs with $r = 2.85$, 3.76, 3.88, 4.46 and 6.41 cm. Inset: D/D_0 of CAP with $r = 6.41$ cm.

New reads:

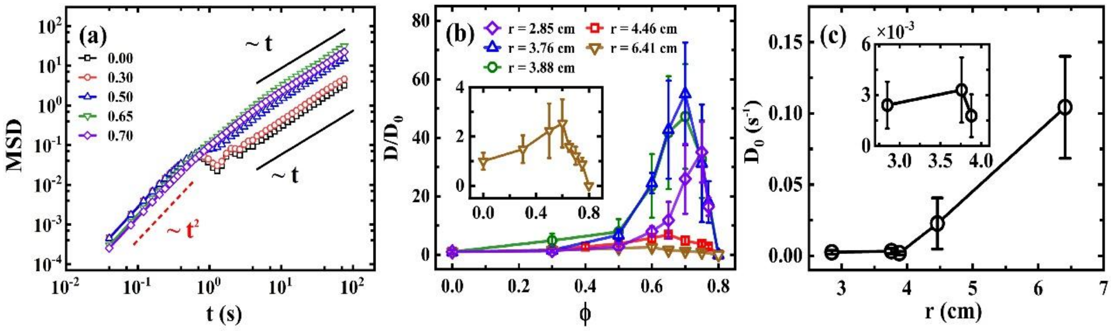

FIG. 2. (a) MSD of a CABP with $r = 4.46$ cm as a function of delay time t at different ϕ. Solid black lines indicate linear scaling, MSD$\sim t$, characteristic of the normal diffusion. (b) The relation between ϕ and D/D_0 for CABPs with $r = 2.85$, 3.76, 3.88, 4.46 and 6.41 cm. Inset: D/D_0 of CAP with $r = 6.41$ cm. (c) Diffusion coefficient D_0 of five CABPs in the absence of obstacles. Inset: D_0 for CABPs with r = 2.85, 3.76, and 3.88 cm.

2. Page 2, right column, first paragraph

It was: "Figure 2(b) plots the normalized diffusion coefficient D/D_0 as a function of ϕ for CAPs with different orbital radii r, where D_0 is the diffusion coefficient in the absence of obstacles."

New reads: "Figure 2(b) plots the normalized diffusion coefficient D/D_0 as a function of ϕ for CABPs with different orbital radii r, where D_0 is the obstacle-free diffusion coefficient shown in Fig. 2(c)."

3. Page 6, right column, the caption of Fig.6

It was:

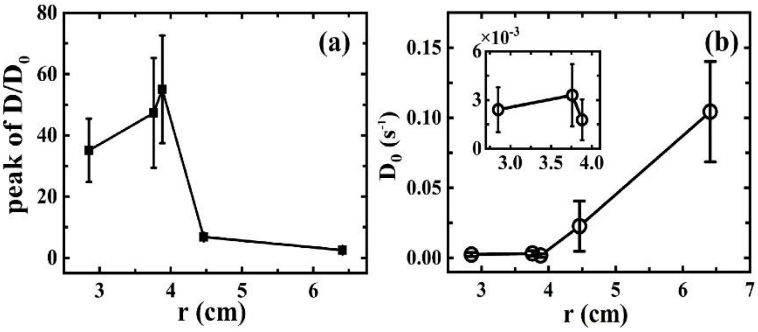

“FIG. 6. (a) The relation between the peak of D/D_0 and r. (b) Diffusion coefficient D_0 for five CAPs in the absence of obstacles. Inset: D_0 for CAPs with $r = 2.85$, 3.76, and 3.88 cm.”

New reads:

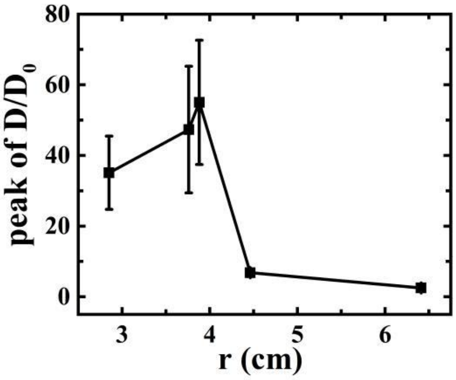

“FIG. 6. The relation between the peak value of D/D_0 and the orbital radius r for CABPs.”

4. Page 6, right column, second paragraph

It was: “Notably, the peak of D/D_0 itself varies nonmonotonically with the orbital radius [Fig. 6(a)]. …... This disparity primarily originates from intrinsic differences in their free-space diffusive capability: the baseline diffusive coefficient D_0 increases with r [Fig. 6(b)], ……”

New reads: “Notably, the peak of D/D_0 itself varies nonmonotonically with the orbital radius [Fig. 6]. …... This disparity primarily originates from intrinsic differences in their free-space diffusive capability: the baseline diffusive coefficient D_0 increases with the orbital radius r [Fig. 2(c)], ……”

Comment (3): The ratio between the Hexbug size and the orbital ratio is not discussed. And maybe more relevant the comparison of the length of both the Hexbug and its trajectory with the obstacles size might play a crucial role.

Response (3): We thank the reviewer for this helpful suggestion. In our experiments, the Hexbug size is fixed (4.3 cm in length and 1.3 cm in width), while the orbital radius *r* is systematically tuned by adjusting the leg asymmetry (Table 1). This design enables the influence of chirality, quantified by *r*, on diffusion dynamics to be isolated from the Hexbug size.

To directly address the relative length scales of the Hexbug, its trajectory, and the obstacles, we performed additional control experiments in which the obstacle diameter was varied to 1.5σ and $2\sigma/3$, with the original obstacle diameter $\sigma = 4.90$ cm, while keeping the CABP orbital radius fixed at $r = 3.76\text{cm}$. As shown in Fig. R4, the normalized diffusion coefficient D/D_0 consistently exhibits a pronounced nonmonotonic dependence on the obstacle area fraction ϕ for all obstacle sizes tested, which only slightly influence the magnitude of diffusion coefficient D/D_0. Notably, the diffusion maximum consistently occurs at $\phi_c = 0.70$. These results demonstrate that the observed nonmonotonic diffusion behavior is robust features of the system, governed primarily by the competition between obstacle-induced motion collimation and the suppression of CABP migration velocity, rather than the specific geometric length ratios. The corresponding results and discussion have been added to the revised manuscript and the Supplementary Material.

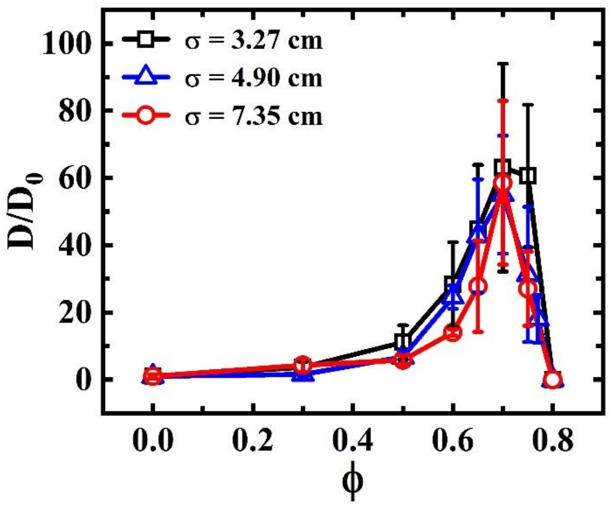

Fig. R4. Normalized diffusion coefficient D/D_0 of CABPs with $r = 3.76\text{cm}$ as a function of obstacle area fraction ϕ for different obstacle diameter σ.

Text changes:

1. Page 3, left column, first paragraph

At the end of the first paragraph, we added the following sentences: "Additional control experiments varying obstacle size, softness, and confinement geometry consistently confirm the robustness of this nonmonotonic diffusion behavior [Supplementary Material]."

Comment (4): How much do the results hinge on the softness of the obstacles? Could experiments be performed also with more rigid objects, such as thin rings?

Response (4): We thank the reviewer for the suggestion regarding the role of obstacle softness. We performed comparative experiments using soft ring obstacles with the thickness of 0.02 mm, and more rigid rings with the thickness of 0.04 mm [Fig. R5]. In both cases, the normalized diffusion coefficient D/D_0 exhibits a pronounced nonmonotonic dependence on the obstacle area fraction ϕ, demonstrating that the emergence of nonmonotonic diffusion enhancement at intermediate crowding does not depend on obstacle softness alone.

Quantitatively, however, the diffusion maximum occurs at a smaller critical area fraction ϕ_c for the more rigid rings, which can be attributed to their reduced deformability of rigid obstacles. Rigid obstacles resist deformation and displacement more strongly, leading to more effective collisions and an earlier suppression of translational motion as ϕ increases. Consequently, the balance between obstacle-induced motion collimation and velocity suppression is reached at lower obstacle densities. These findings indicate that while the nonmonotonic diffusion originates from a generic competition between motion collimation and migration suppression in displaceable media, obstacle softness modulates the transport efficiency and the location of the diffusion maximum. This sensitivity highlights the relevance of soft and deformable obstacles for modeling active transport in biologically relevant setting, where environmental structures are typically soft rather than rigid. The corresponding results and discussion have been added to the updated manuscript and the Supplementary Material.

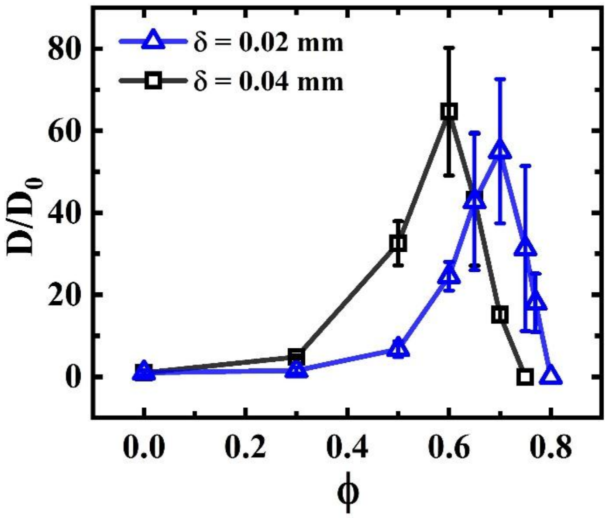

Fig. R5. Normalized diffusion coefficient D/D_0 versus obstacle area fraction ϕ for a CABP with $r = 3.76\text{cm}$, obtained with ring obstacles of thickness $\delta = 0.02\text{ mm}$ (blue) and 0.04 mm (black).

Text changes:

1. Page 3, left column, first paragraph

At the end of the first paragraph, we added the following sentences: "Additional control experiments varying obstacle size, softness, and confinement geometry consistently confirm the robustness of this nonmonotonic diffusion behavior [Supplementary Material]."

Comment (5): Eq. (3) seems to be obtained in the obstacle-free space case, looking at the trajectories in Fig.7a it seems questionable.

Response (5): In obstacle-free conditions, chiral active Brownian particles undergo simultaneous self-propulsion and autonomous rotation, leading to spiral or circular trajectories in real space, as shown in Fig. 1(c). Although these trajectories [Fig. 7(a)] appear spatially confined, our analysis is performed in a polar coordinate system centered at the disk origin [Fig. 1(a)], where the CABP dynamics are characterized by the angular coordinate θ. In this representation, θ is effectively unbounded subject to periodic boundary conditions, so the CABP motion along the angular direction corresponds to a stochastic angular random walk. Consequently, while the real-space trajectories in Fig. 7(a) appear spatially confined, the angular θ exhibits diffusive behavior in obstacle-free space case and can be described by Eq. (3).

To prevent potential confusion, the distinction between real-space confinement and angular diffusion has been clarified explicitly in the revised manuscript.

Text changes:

Page 5, right column, third paragraph

It was: "Theoretically, the effective diffusion coefficient of a CAP in obstacle-free space can be expressed as [53] ……"

New reads: "In the annular channel geometry, CABP motion along the azimuthal direction θ is effectively unconfined and experiences periodic boundary conditions. Consequently, the measured angular displacement $\Delta\theta$ can exceed 2π. Under obstacle-free conditions, the effective diffusion coefficient of a CABP can therefore be expressed theoretically as [Phys. Rev. E. 78, 020101 (2008), Phys. Rev. E. 94, 062120 (2016), 63] ……"

Comment (6): Then the applicability of Eq. (3) is extended to complex media, which is not obvious either, also regarding the trajectories in Fig.7. The authors should extensively comment on this.

Response (6): We thank the reviewer for this kindness suggestion. The applicability of Eq. (3) is extended to complex media by reinterpreting all dynamical parameters as effective and environment-dependent quantities.

In the presence of obstacles, CABP dynamics are strongly modified by frequent CABP–obstacle collisions. While the substrate friction remains essentially constant, additional effective friction arises from CABP–obstacle collisions and depends on the obstacle area fraction ϕ. As ϕ increases, collisions increasingly suppress reorientation events, making it more difficult for CABPs to alter their direction of motion. This leads to enhanced directional persistence, reflected by the increase of $t_{\mathrm{m}}/t_{\mathrm{tot}}$ and interpreted as an increase in effective rotational friction $\gamma_{\mathrm{r}}(\phi)$. Similarly, the reduction of the migration speed v reflects the enhancement of translational friction, captured by $\gamma_t(\phi) \propto v_0/v$. To quantify these obstacle-induced effects, we introduce the empirical relations $\gamma_{\mathrm{r}}(\phi) \propto t_{\mathrm{m}}/t_{\mathrm{tot}}$ and $\gamma_t(\phi) \propto v_0/v$, linking the effective friction coefficients to experimentally measurable observables. Substituting these effective ϕ-dependent parameters into Eq. (3) yields a generalized diffusion expression that reproduces the experimentally observed nonmonotonic diffusion behavior with the obstacle area fraction ϕ.

In obstacle-free space [Fig. 7(a) and Fig. 7(c)], CABPs with different orbital radii r follow circular trajectories, corresponding to their baseline diffusivity D_0, which increases with r [Fig. 2(c) in the updated manuscript]. At higher obstacle densities [Fig. 7(b) and Fig. 7(d)], the trajectories instead exhibit extended, nearly straight segments, indicating obstacle-induced collimation and enhanced directional persistence. This transition directly underlies the diffusion enhancement captured by the generalized framework. Notably, while CABPs with larger r exhibit higher intrinsic diffusivity in free space, their maximum diffusivities in obstacles environments become comparable to those with smaller r [Fig. 7(b) and Fig. 7(d)], demonstrating that obstacle-induced collimation disproportionately enhances the transport of small-radius CABPs with intrinsically weaker motility. Consequently, soft-ring obstacles not only promote diffusion overall but also induce a pronounced, radius-dependent modulation of transport efficiency.

In the revised manuscript, we have clarified that Eq. (3) is applied to complex media through an effective, ϕ-dependent reinterpretation of its parameters, and the corresponding CABP trajectories in Fig. 7 have also been discussed explicitly.

Text changes:

1. Page 5, right column, third paragraph

It was: "Here, Eq. (3) remains applicable ...... The relations are given by $\gamma_r(\phi) \propto t_{\mathrm{m}}/t_{\mathrm{tot}}$ and $\gamma_t(\phi) \propto v_0/v$."

New reads: "For a CABP moving in obstacle-free space, the thermal translational diffusion coefficient is given by $D_t^T = k_B T/\gamma_t^0$. The rotational relaxation time (i.e., the persistence time) is defined as $\tau_r = 1/D_r = \gamma_r^0/(k_B T)$, where D_r is the rotational diffusion coefficient extracted from the mean-squared angular displacement (MSAD) or orientation autocorrelation [Soft Matter 12, 4584 (2016), J. Chem. Phys. 121, 11322 (2004)]. The translational and angular velocity are $v_0 = F_d/\gamma_t^0$ and $\omega_0 = T_d/\gamma_r^0$, respectively, with γ_t^0 and γ_r^0 being the translational and rotational friction coefficients in obstacle-free space, and F_d and T_d the driving force and torque acting on the particle.
Accordingly, the effective diffusion coefficients in obstacle-free space can be approximated as

$$D_0 = k_B T/\gamma_t^0 + \frac{{F_d}^2 \gamma_r^0/{\gamma_t^0}^2}{2k_B T\left[1+(\frac{T_d}{k_B T})^2\right]} \tag{4}$$

The environment with increasing obstacle area fraction ϕ simultaneously modifies translational and rotational dynamics. Frequent collisions suppress the migration speed, thereby enhancing the effective translational friction $\gamma_t(\phi)$, while the obstacle-induced alignment enhances orientational persistence, effectively reducing the rotational diffusion coefficient and leading to an increased effective rotational friction $\gamma_r(\phi)$. These effects motivate us to treat both friction coefficients as ϕ-dependent. Experimentally, they are captured by the empirical relations $\gamma_r(\phi) \propto t_{\mathrm{m}}/t_{\mathrm{tot}}$ and $\gamma_t(\phi) \propto v_0/v$, which quantify the enhancement of directional persistence and the suppression of migration speed, respectively. By substituting these relations into Eq. (4) yields the generalized diffusion coefficient in obstacle-rich environments,

$$D = k_B T/\gamma_t(\phi) + \frac{{F_d}^2 \gamma_r(\phi)/\gamma_t(\phi)^2}{2k_B T\left[1+(\frac{T_d}{k_B T})^2\right]}. \tag{5}$$

Since the thermal translational term $D_t^T = k_B T/\gamma_t(\phi)$ is negligibly compared with the activity-induced contribution, the effective diffusion coefficients of particles in the presence and absence of obstacles can be approximated as

$$D \approx \frac{{F_d}^2 \gamma_r(\phi)/\gamma_t(\phi)^2}{2k_B T\left[1+(\frac{T_d}{k_B T})^2\right]}, \tag{6}$$

$$D_0 \approx \frac{{F_d}^2 \gamma_r^0/{\gamma_t^0}^2}{2k_B T\left[1+(\frac{T_d}{k_B T})^2\right]}. \tag{7}$$

Consequently, the normalized diffusion coefficient becomes

$$\frac{D}{D_0} = \frac{\gamma_r(\phi){\gamma_t^0}^2}{\gamma_t^2(\phi)\gamma_r^0} \tag{8}$$”

2. Page 6, right column, second paragraph

It was: “This disparity primarily originates from intrinsic differences in their free-space diffusive capability: the baseline diffusive coefficient D_0 increases with *r* [Fig. 6(b)], as illustrated by representative trajectories in free space [Fig. 7(a) and Fig. 7(c)]. When interacting with soft-ring obstacles, however, their maximum diffusive capabilities converge [Fig. 7(b) and Fig. 7(d)], indicating that the obstacle-induced collimation effect disproportionately enhances the transport of small-radius CAPs with intrinsically weaker motility.”

New reads: “This disparity primarily originates from intrinsic differences in their free-space diffusive capability: the baseline diffusive coefficient D_0 increases with the orbital radius r [Fig. 2(c)], as illustrated by representative free-space trajectories of CABP with r=6.41 cm [Fig. 7(a)] and 2.85 cm [Fig. 7(c)] at ϕ = 0.0. In contrast, in the presence of soft-ring obstacles, the maximum diffusive capabilities attained by CABPs with r=6.41 cm [Fig. 7(c)] and 2.85 cm [Fig. 7(d)] become comparable. Consequently, the relative diffusion enhancement is significantly larger for CABPs with smaller orbital radius (r = 2.85 cm), indicating that the obstacle-induced collimation disproportionately enhances the transport of CABPs with different r."

Comment (7): The measurement of diffusion is of central importance to this work, but judging from the results in Fig2a it is not completely clear that the linear regime has been properly reached. It could be that the measurements are too short, or that there is another mechanism preventing this. Maybe plot MSD/t vs. t would help in this respect, and also to clarify the origin of the really large error bars in Fig2b.

Response (7): We thank the reviewer for this helpful suggestion. In our experiments, the characteristic orbital period of CABPs to range from 0.74 to 1.61 s. When analyzed in polar coordinates centered at the disk origin, the mean-squared angular displacement evolves from a short-time ballistic regime to a well-defined linear diffusive regime at long times [Nat. Commun. 15, 1406 (2024)], as the CABPs complete many orbital cycles and loses their initial directional memory well before the end of the experimental measurement window, which extends up to approximately 10 minutes. The diffusion coefficient D was therefore extracted from this long-time linear regime, as shown in Fig. R6.

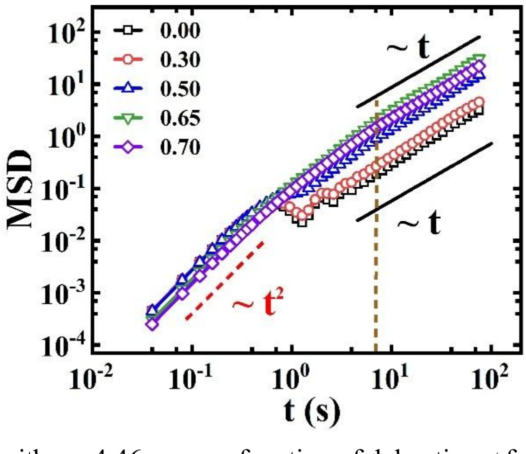

Fig. R6. MSD of a CABP with r = 4.46 cm as a function of delay time t for different ϕ. Solid black lines indicate linear scaling, MSD$\sim t$, characteristic of the normal diffusion. The brown dotted line corresponds to t=7s.

To further clarify that the diffusive regime is properly reached, we followed the reviewer's suggestion and added plots of MSD/t versus delay time t [Fig. R7 (a)]. These plots show that MSD/t converges to a smooth region after several orbital periods, confirming that the linear regime of the MSD is properly reached within the measurement duration. In addition, we analyzed $\Delta\mathrm{MSD} = \mathrm{MSD}(t) - \mathrm{MSD}(t_0)$ as a function of $\Delta t = t - t_0$ with $t_0 = 7$ s [Fig. R7 (b)]. This procedure minimizes the influence of early-time transient dynamics and show that $\Delta\mathrm{MSD}/\Delta t$ reaches a stable plateau over an extended time window, further confirming the validity of the linear diffusion regime.

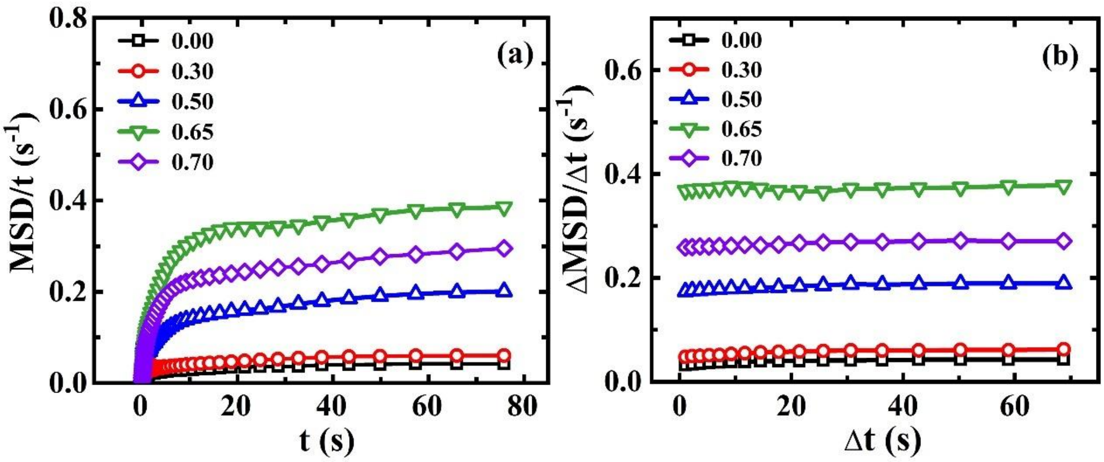

Fig. R7. (a) MSD/t of a CABP with r = 4.46 cm as a function of the delay time *t* at different ϕ. (b) $\Delta\mathrm{MSD}/\Delta t$ of the same CABP as a function of Δt for different ϕ.

For each CABP and ϕ, the diffusion coefficient was obtained from 3-7 independent measurements under identical conditions. In each measurement, trajectories were recorded for approximately 10 minutes at 25 frames/s, yielding thousands of data points per trajectory. The error bars in Fig. 2(b) arises from the variability of the extracted diffusion coefficients across these independent measurements. The corresponding analyses and clarifications have been added to the revised manuscript.

Text change:

1. Page 3, Fig.2(a)

It was:

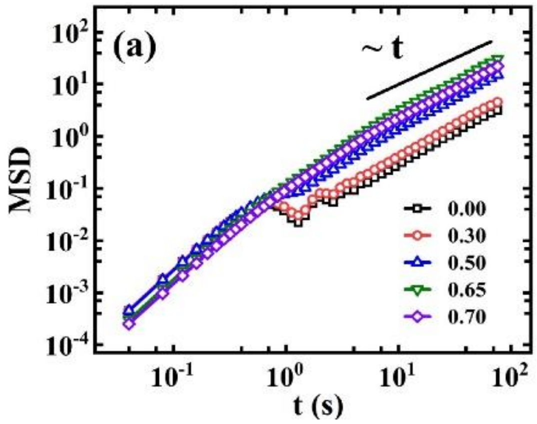

FIG. 2. (a) The MSD of a CAP with $r = 4.46$ cm as a function of delay time t at different ϕ.

New reads:

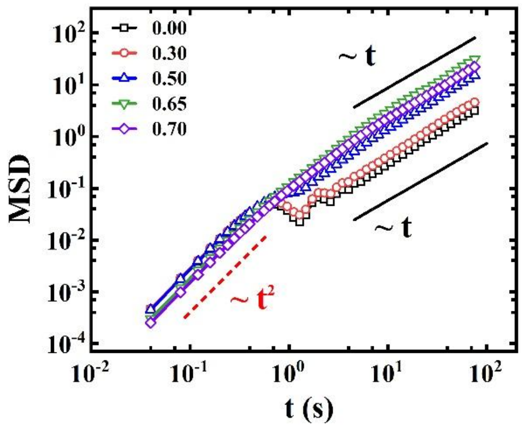

FIG. 2. (a) MSD of a CABP with $r = 4.46$ cm as a function of delay time t at different ϕ. Solid black lines indicate linear scaling, $\mathrm{MSD} \sim t$, characteristic of the normal diffusion.

2. Page 7, right column, the section of Methods

It was: "Each experimental run was limited to 15 minutes to ensure stable propulsion speeds, and batteries were replaced before each run to maintain consistency across trials [30]. A red marker was affixed to the back of each robot to facilitate accurate image-based tracking. CAP trajectories were recorded by a camera at 25 frames/s and subsequently extracted using particle recognition and tracking software."

New reads: "Each experimental run was limited to 15 minutes to ensure stable propulsion speeds, and batteries were replaced before each run to maintain consistency across trials [30]. Images of the sample were recorded with approximately 10 minutes by a camera at 25 frames/s. For each CABP and obstacle area fraction ϕ, 3-7 independent measurements were performed under identical conditions, yielding an ensemble of long-time diffusion coefficients D. The error bars shown in Fig. 2(b) represent the statistical variability across these measurements and increase near the critical density ϕ_c, where CABPs stochastically switch between trapped and migrating states with the variable relative duration of these states. CABP trajectories were extracted using particle recognition and tracking software, aided by a red marker affixed to the back of each robot to facilitate accurate image-based tracking."

3. Page 2, left column, the last paragraph

It was: "Figure 2(a) shows the mean square displacement (MSD) in a polar coordinate system centered at the disk origin, evaluated at different time interval t, $\mathrm{MSD} = \langle[\theta(t_0+t)-\theta(t_0)]^2\rangle = 2Dt$, from which the longtime diffusion coefficient D can be extracted."

New reads: "The dynamics of CABPs are quantified by the mean square displacement (MSD) of the angular coordinate θ, evaluated in a polar coordinate system centered at the disk origin for different time interval t [Fig. 2(a)]. At short time, the MSD exhibits a ballistic scaling, $\mathrm{MSD} \propto t^2$, reflecting the circular motion. After many orbital cycles, it crosses over to a normal diffusion regime with $\mathrm{MSD} \propto t$ at long times [Nat. Commun. 15, 1406 (2024)], from which the long-time diffusion coefficient D is extracted via $\mathrm{MSD} = \langle[\theta(t_0+t)-\theta(t_0)]^2\rangle = 2Dt$."

Comment (8): The influence of the employed confinement geometry is also barely discussed.
8a -- Would the results be very different if the confinement would be simply circular, $R_{in} = 0$
8b -- or if there would not be any confinement, $R_{out} \gg r$?
8c -- for $r \cong R_{in}$, could there be some sort of particular enhancement?
8d -- could experiments in other geometries be performed?
8e -- could some more insights on how the results would translate to a different geometry be provided?

Response (8a): We thank the reviewer for raising this question concerning the role of confinement geometry. We performed additional control experiments in a simply confinement with $R_{\mathrm{in}} = 0$ cm, where CABPs move within a fully circular domain. As shown in Fig. R8, the normalized diffusion coefficient D/D_0 still exhibits a pronounced nonmonotonic dependence on the obstacle area fraction ϕ, in qualitative agreement with the behavior observed in the annular geometry. This result indicates that the nonmonotonic diffusion enhancement is not specific to the annular confinement, but instead arises from the intrinsic interplay between CABP dynamics and obstacle interactions. The corresponding analysis has been added to the revised manuscript and the Supplementary Material.

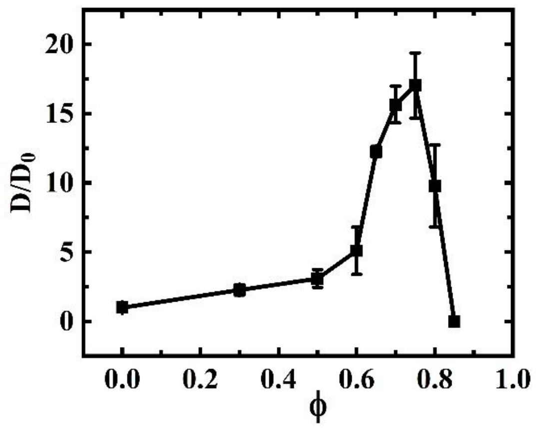

Fig. R8. The normalized diffusion coefficient D/D_0 for CABP with r = 3.76 cm as a function of ϕ without inner boundary ($R_{\text{in}} = 0$ cm).

Response (8b): Although the system size is relatively small, boundary effects do not significantly influence the transport behavior reported here. Both the inner and outer boundaries are composed of petal-shaped arc segments, which effectively suppress persistent sliding along the boundaries and thus minimize boundary-dominated transport [Nat. Commun. 5, 4688 (2014)]. Moreover, our analysis focuses on one-dimensional angular diffusion along the azimuthal direction θ. In this annular geometry, radial motion is confined, while diffusion in θ effectively experiences periodic boundary conditions. Provided that R_{out} is much larger than the particle orbital radius r, variations in the radial boundaries do not qualitatively affect the observed nonmonotonic diffusion. Consequently, the observed nonmonotonic transport behavior is governed by CABP–obstacle interactions rather than boundary-induced effects.

Response (8c): We thank the reviewer for raising this interesting question. We performed additional experiments with a reduced inner boundary, setting $R_{\text{in}} = 3.76$ cm to match the orbital radius of a representative CABP. As shown in Fig. R9, the normalized diffusion coefficient D/D_0 continues to exhibit a pronounced nonmonotonic dependence on the obstacle area fraction ϕ, without any additional enhancement relative to the original annular geometry. This result indicates that no special transport enhancement emerges from the condition $r = R_{\text{in}}$. Instead, the observed nonmonotonic diffusion behavior remains a robust consequence of CABP-obstacle interactions, rather than an effect arising from the specific choice of confinement geometry.

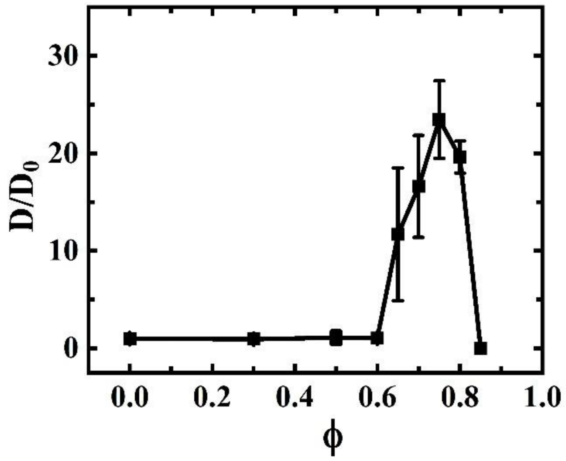

Fig. R9. Normalized diffusion coefficient D/D_0 as a function of ϕ for CABP with r = 3.76 cm, measured in an annular confinement with inner boundary radius $R_{\text{in}} = 3.76$ cm.

Response (8d): We conducted additional experiments in a square-shaped confinement [Fig. R10], with an outer boundary of 70 cm and an inner boundary of 14.5 cm, while keeping the accessible channel area identical to that of the annular configuration. As shown in Fig. R11, the normalized diffusion coefficient D/D_0 continues to exhibit a pronounced nonmonotonic dependence on the obstacle area fraction ϕ, with a maximum occurring at an intermediate density $\phi_c = 0.70$. These results demonstrate that the observed nonmonotonic diffusion enhancement is not specific to annular confinement, but instead reflects a generic transport mechanism arising from the competition between obstacle-induced motion collimation and migration suppression in reconfigurable disordered media.

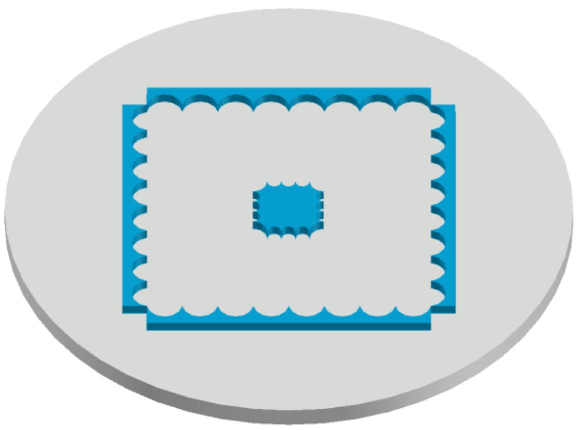

Fig. R10. Experimental setup with square-shaped confinement boundaries.

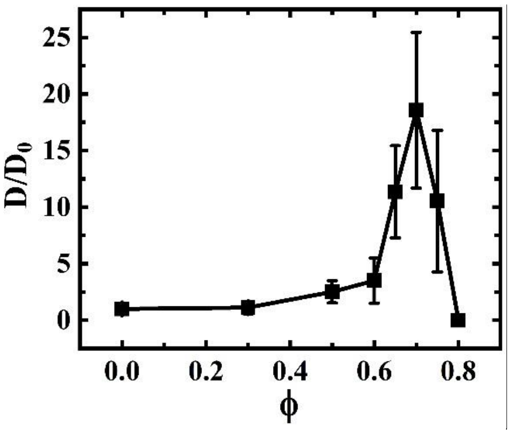

Fig. R11. The relation between ϕ and D/D_0 for a CAP with r = 3.76 cm under square confinement with an outer boundary of 70 cm and an inner boundary of 14.5 cm.

Response (8e): Our additional experiments show that the observed nonmonotonic diffusion enhancement is robust to variations in confinement geometry. The characteristic nonmonotonic dependence of the normalized diffusion coefficient on obstacle density persists across different geometrical configurations, indicating that the underlying mechanism is not determined by specific boundary shapes. This behavior arises from a generic competition between obstacle-induced motion collimation and migration suppression, which is governed by CABP–obstacle interactions and is therefore expected to remain effective across different geometries.

Text changes:

1. Page 3, left column, first paragraph

At the end of the first paragraph, we added the following sentences: "Additional control experiments varying obstacle size, softness, and confinement geometry consistently confirm the robustness of this nonmonotonic diffusion behavior [Supplementary Material]."

2. Page 5, right column, third paragraph

It was: "Theoretically, the effective diffusion coefficient of a CAP in obstacle-free space can be expressed as [53] ……"

New reads: "In the annular channel geometry, CABP motion along the azimuthal direction θ is effectively unconfined and experiences periodic boundary conditions. Consequently, the measured angular displacement $\Delta\theta$ can exceed 2π. Under obstacle-free conditions, the effective diffusion coefficient of a CABP can therefore be expressed theoretically as [Phys. Rev. E. 78, 020101 (2008), Phys. Rev. E. 94, 062120 (2016), 63] ……”

Comment (9): What is the advantage of analyzing the self-overlap function instead of the more traditional orientation autocorrelation function?

Response (9): The standard orientation autocorrelation function of the CABP's orientation, $C_\theta(\mathrm{t})=\langle\vec{e}(t_0)\cdot\vec{e}(t+t_0)\rangle = e^{-t/\tau_r}$, provides an unambiguous measure of rotational decorrelation, with the rotational diffusion coefficient $\tau_r = 1/D_r$ in two dimensions [Eur. Phys. J. E 40, 23 (2017)]. For completeness, the corresponding values of τ_r and D_r for CABPs in obstacle-free space are reported in Table 1 of the updated manuscript.

The advantage of analyzing the self-overlap function Q(t) is that it is specifically designed to resolve local confinement and dynamical heterogeneity, which are not directly accessible from $C_\theta(\mathrm{t})$. In obstacle environments, CABP motion alternates between trapped and migratory states. While $C_\theta(\mathrm{t})$ averages over all orientations and primarily reflects rotational diffusion, Q(t) probes whether the particle remains within a prescribed angular window over time, thereby directly quantifying the persistence of local trapping. This approach has been widely used to characterize cage effects and heterogeneous dynamics [Nat. Commun. **11**, 2581 (2020); Proc. Natl. Acad. Sci. USA **116**, 22977 (2019)].

In this sense, $C_\theta(t)$ captures rotational relaxation, whereas Q(t) provides a more appropriate tool for identifying local trapping and dynamical heterogeneity, which is the central focus of the present study.

Comment (10): How are $\mathbf{F_d}$ and $\mathbf{T_d}$ evaluated?

Response (10): F_d and T_d denote the intrinsic self-propulsion force and torque generated by the internal actuation of CABP and are therefore independent of the obstacle density. They are evaluated from the experimentally measured free-space translational velocity v_0 and angular velocity ω_0 via $F_d = \gamma_t^0 v_0$ and $T_d = \gamma_r^0 \omega_0$, respectively, where γ_t^0 and γ_r^0 are the translational and rotational friction coefficients in obstacle-free space.

Comment (11): In line 177 the authors make an unclear connection between the system heterogeneity and to supercooled liquids.

Response (11): The original reference to supercooled liquids was intended only to indicate that similar measures of dynamical heterogeneity are used across different systems. However, this comparison may be unclear and potentially misleading in the original context. To avoid confusion, we have removed the explicit reference to supercooled liquids and discussed the dynamical heterogeneity of the CABP system directly, focusing exclusively on the phenomena observed in our experiments.

Text changes:

Page 4, right column, first paragraph

It was "……, indicative of significant dynamical heterogeneity consistent with the behaviors observed in supercooled liquids [52]."

New reads: "……, indicative of significant dynamical heterogeneity in the motion of CABPs within obstacle-rich environments."

Comment (12): The migration time, first appearing in line 192 is not defined before and not afterwards.

Response (12): We thank the reviewer for pointing out the migration time was not clearly defined in the original manuscript. The migration time t_m is defined as the cumulative duration that a CABP spends in the migration state during a single experimental trial, while the total time t_{tot} denotes the total duration of that run. The corresponding definitions have been added in the updated manuscript.

Text changes:

1. Page 3, right column, first paragraph

It was: "The CAP is defined as being in the trapped state if it remains within a radius $\mathrm{R_c}$ from its initial position and completes at least two rotations, with R_c determined from the characteristic confinement scale at a given ϕ."

New reads: "The CABP is defined as being in the trapped state if it remains within a circular region of radius R_c centered at its initial position and completes at least two rotations. The confinement radius R_c is determined by the characteristic confinement scale at a given obstacle area fraction ϕ and is defined as the average diameter of all identified trapped regions [the details in the Supplementary Material]. Otherwise, if the residence time within the R_c region is shorter than two rotational periods, the CABP is classified as being in the migration state."

2. Page 4, right column, second paragraph

It was: "Figures 4(a)-(e) present the normalized migration time t_m/t_{tot} and normalized velocity v/v_0 for various CAPs as functions of the obstacle area fraction ϕ, where t_{tot} is the duration of a single experimental trial."

New reads: "Figures 4(a)-(e) present the normalized migration time t_m/t_{tot} and normalized velocity v/v_0 for various CABPs as functions of the obstacle area fraction ϕ. Here, the migration time t_m is defined as the cumulative duration that a CABP spends in the migration state during a single experimental run, and t_{tot} denotes the total duration of that run. The velocities v and v_0 are obtained by averaging the frame-to-frame displacement divided by the frame interval over the full trajectory in the presence and absence of obstacles, respectively."

Comment (13): I guess that the velocities are measured from the MSD (please specify), but how are the migration times obtained? I understand that the manuscript specifies migration time and relaxation times as two different quantities.

Response (13): We thank the reviewer for this important clarification. The CABP velocities are not measured from the MSD. Instead, they are calculated directly from the tracked trajectories by calculating the displacement between consecutive frames divided by the frame interval. The reported mean velocity is then obtained by averaging these inter-frame velocities over the entire trajectory, both in the absence (v_0) and presence (v) of obstacles.

The migration time t_m is determined through a state-based classification of the CABP dynamics. Specifically, each trajectory is segmented into trapped and migrating states according to the criteria defined in the manuscript, and t_m is defined as the cumulative duration spent in the migrating state during a single experimental run. The total time t_{tot} is simply the duration of that run. In contrast, the relaxation time τ characterizes a distinct dynamical process and is extracted from the decay of the two-point overlap correlation function Q(t), defined as the time at which Q(t) decays to 1/e.

Text changes:

1. Page 4, right column, second paragraph

It was: "Figures 4(a)-(e) present the normalized migration time t_m/t_{tot} and normalized velocity v/v_0 for various CAPs as functions of the obstacle area fraction ϕ, where t_{tot} is the duration of a single experimental trial."

New reads: "Figures 4(a)-(e) present the normalized migration time t_m/t_{tot} and normalized velocity v/v_0 for various CABPs as functions of the obstacle area fraction ϕ. Here, the migration time t_m is defined as the cumulative duration that a CABP spends in the migration state during a single experimental run, and t_{tot} denotes the total duration of that run. The velocities v and v_0 are obtained by averaging the frame-to-frame displacement divided by the frame interval over the full trajectory in the presence and absence of obstacles, respectively."

Comment (14): The four plots in Fig 4 might be more informative if they would all be presented in a single plot. The functions used to fit Fig.4b should be specified in the caption.

Response (14): We thank the reviewer for this constructive suggestion. We explored presenting all datasets in a single plot to facilitate direct comparison. However, we found that combining all curves corresponding to different CABPs [Fig. R12] led to substantial visual overcrowding, which obscured the individual trends and reduced readability. We therefore retained a multi-plot representation, which allows the behavior of each CABP with distinct orbital radius *r* to be clearly resolved while preserving meaningful comparisons. In the revised manuscript, we have explicitly specified the fitting functions in the caption of Fig. 4 to improve clarity.

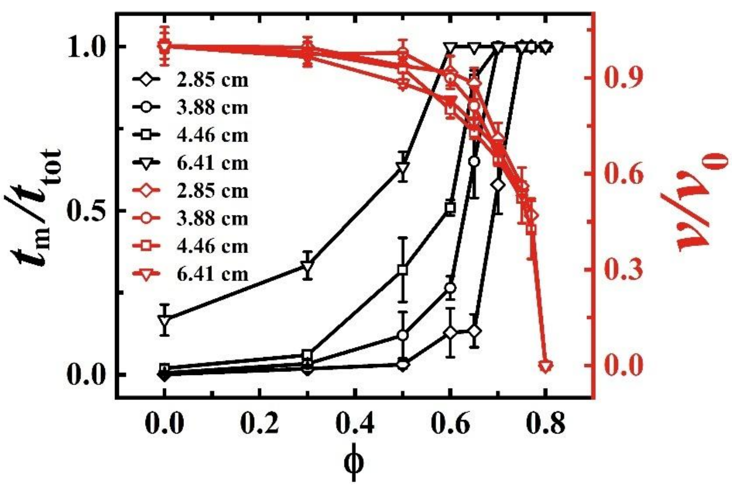

Fig. R12. Normalized migration time t_m/t_{tot} (black samples) and velocity v/v_0 (red samples) of CABPs with different *r* as functions of obstacle area fraction ϕ.

Text changes:

Page 4, the caption of Fig. 4

It was: "Normalized migration time t_m/t_{tot} (black triangles) and velocity v/v_0 (red circles) of CAPs with different *r* as functions of obstacle area fraction ϕ. Green and blue dashed lines in (b) represent fits for t_m/t_{tot} and v/v_0, respectively."

New reads: "Normalized migration time t_m/t_{tot} (black triangles) and normalized velocity v/v_0 (red circles) of CABPs with different *r* as functions of obstacle area fraction ϕ. Green and blue dashed lines in (b) represent fits to the data using empirical functions $t_m/t_{tot} = A_1 e^{b_1 \phi}$ and $v/v_0 = 1/(y_2 + A_2 e^{b_2 \phi})$, respectively."

Comment (15): The fits performed in Fig. 4b could be also extended to the other 4 sets of parameters. Is there a reason why this is not done? Would the fitted values be very different?

Response (15): We thank the reviewer for this constructive suggestion. The same fitting procedure has been extended to all CABPs with different orbital radii *r* [Fig. R13], and the corresponding fitting parameters vary with *r* [Table R2], reflecting differences in the dynamics of the CABPs. Importantly, however, the same functional form remains applicable across all cases. This extended analysis confirms that the empirical functional forms consistently capture the competition between migration enhancement and velocity suppression for all CABPs studied. To maintain clarity and focus in the main text, these additional fits and corresponding parameter tables are provided in the Supplementary Material.

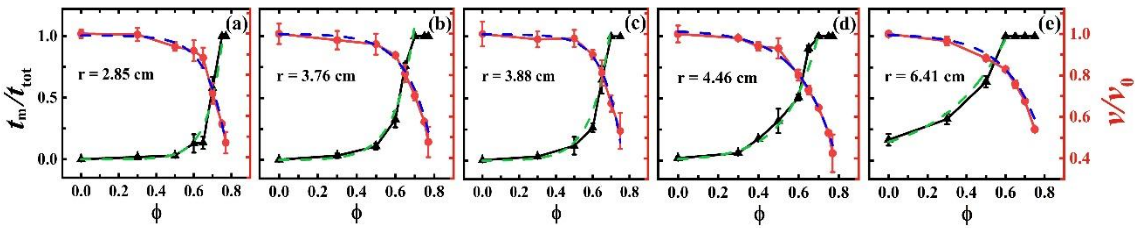

Fig. R13. Normalized migration time t_m/t_{tot} (black samples) and velocity v/v_0 (red circles) of CABPs with different *r* as functions of obstacle area fraction ϕ. The dashed lines represent fits to the experimental data using the empirical functions $t_m/t_{tot} = A_1 e^{b_1 \phi}$ (green) and $v/v_0 = 1/(y_2 + A_2 e^{b_2 \phi})$ (blue), respectively.

r (cm)	2.85	3.76	3.88	4.46	6.41
A_1	8×10^{-5}	0.001	0.001	0.01	0.15
b_1	12.5	10	10	6.67	3.125
y_2	1	1	1	1	1
A_2	2.0×10^{-4}	4.5×10^{-5}	4.6×10^{-4}	5.6×10^{-4}	3.6×10^{-3}
b_2	11	13	10	10	7

Table R2. Fitting parameters A_1, b_1, y_2, A_2, and b_2 for CABPs with different radii *r*.

Text changes:

1. Page 6, right column, first paragraph

Following the sentence "On this basis, the theoretical prediction from Eq. (6), presented in the inset of Fig. 5(b), successfully reproduces the trends observed in both the experimental diffusion coefficient D/D_0 [blue triangles in Fig. 2(b)] and $v^2 t_m/(v_0^2 t_{tot})$ [blue triangles in Fig. 5(a)].", we added the following sentences: "The same empirical fitting functions and scaling analysis were applied to four additional CABPs with different orbital radii *r*, all of which show consistent agreement with the observed trends [Supplementary Material]."

Comment (16): I am not sure I properly understand, but it seems that Fig. 5b corresponds to the fits obtained and already shown in Fig 4b. If I am right, I am not sure why this is repeated here. Why are symbols used in the inset and not in the main plot? And would it be possible to plot the values in Fig 2b together with the relation obtained from the velocities and migration times.

Response (16): We thank the reviewer for the helpful suggestions. Although Fig. 5(b) is constructed using the fitted quantities shown in Fig. 4(b), its purpose is fundamentally different and not redundant. Figure 4(b) presents independent empirical fits of the normalized migration time t_m/t_{tot} and velocity ratio v/v_0 as functions of ϕ. By contrast, Fig. 5(b) combines these independently extracted quantities through the scaling relation, $\frac{D}{D_0} = \frac{\gamma_r(\phi)\gamma_t^{0^2}}{\gamma_t^2(\phi)\gamma_r^0}$, to obtain an estimate of the normalized diffusivity. Figure 5(b) therefore serves as an internal consistency check of the scaling framework by directly comparing this estimate with the experimentally measured diffusion.

Regarding the plotting style, symbols were omitted in the inset of Fig. 5(b) to improve visual clarity and to emphasize the scaling trend rather than individual data points, consistent with the main plot [Fig. R14].

Following the reviewer's suggestion, we have additionally overlaid the experimental diffusion data from Fig. 2(b) with the diffusion estimate constructed from the combined normalized rotational and translational friction coefficients, γ_r/γ_r^0 and $(\gamma_t^0/\gamma_t)^2$, as shown in Fig. R15. This comparison shows that the scaling framework successfully captures the nonmonotonic dependence on ϕ and correctly identifies the location of the diffusion maximum of CABPs in complex media, although quantitative deviations between the estimated and measured values remain.

We speculate that these quantitative deviations arise from the simplifying assumption that the influence of the obstacle background can be fully absorbed into effective friction coefficients. In practice, obstacle–CABP collisions may also generate additional stochastic contributions, analogous to noise, which are expected to be active and colored rather than equilibrium thermal noise. The situation is reminiscent of colloidal particles moving in a molecular fluid, where the surrounding medium contributes both friction and noise to the particle dynamics. Moreover, such active and maybe environment-dependent noise are difficult to incorporate within a simple scaling description. In the present analysis, we therefore retain only the frictional effects and neglect these noise contributions. Importantly, this approximation does not affect the qualitative trends or the predicted location of optimal diffusion enhancement.

The purpose of the scaling analysis is thus to rationalize the observed trends and extrema, rather than to reproduce an independent quantitative prediction of the absolute magnitude of D/D_0. Corresponding clarifications have been added to the revised manuscript and the Supplementary Material.

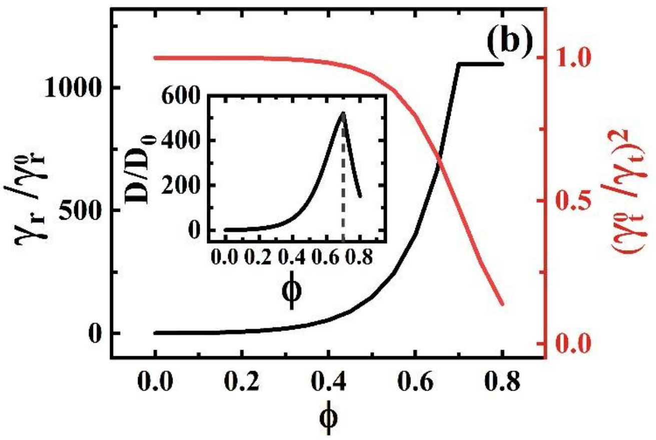

Fig. R14. The empirical predictions of the normalized rotational friction coefficient (γ_r/γ_r^0) (black line) and translational friction coefficient $(\gamma_t^0/\gamma_t)^2$ (red line) of a CABP with *r* = 3.76 cm, as functions of obstacle area fraction ϕ. Inset: The empirical predicted normalized diffusion coefficient D/D_0 versus ϕ, exhibiting a peak at ϕ = 0.70.

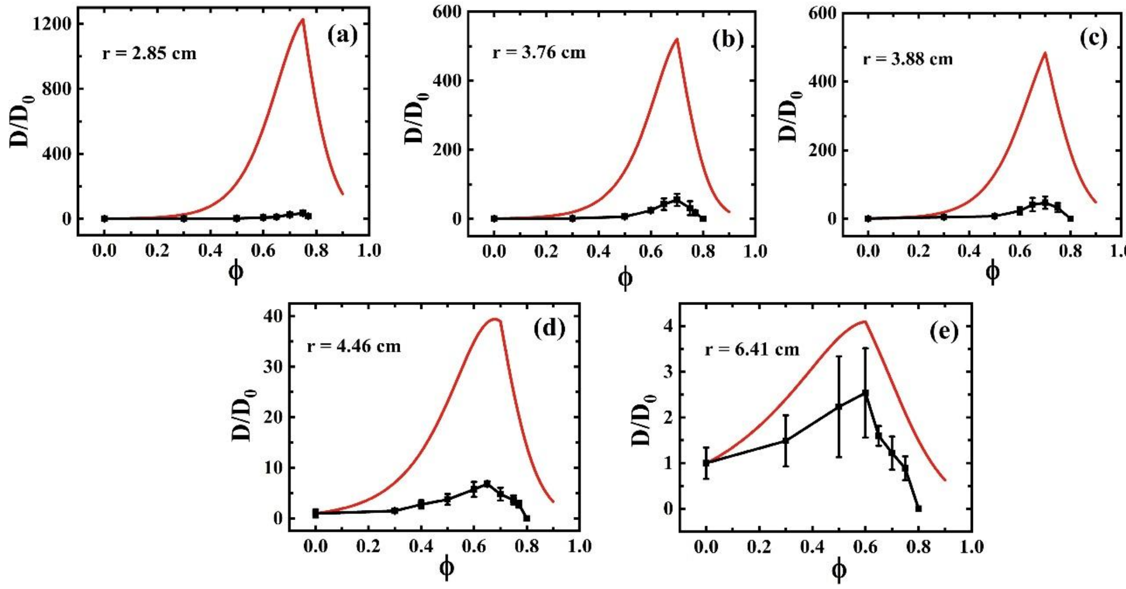

Fig. R15. The empirical prediction (red line) and experimental data (black line) of the normalized diffusion coefficient D/D_0 for CABPs with orbital radius *r*, as a function of obstacle area fraction ϕ.

Text changes:

1. Page 5, Figure 5(b)

It was:

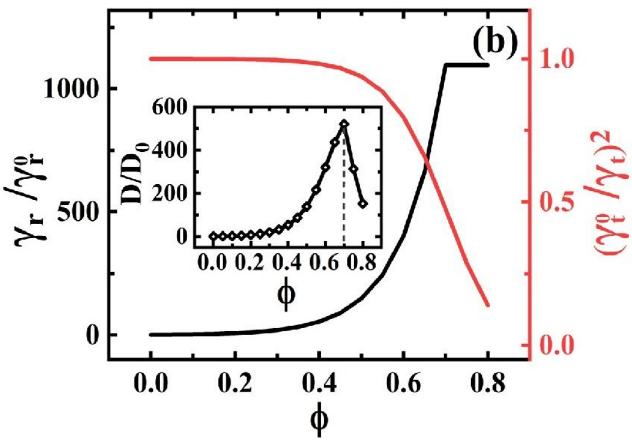

(b) Theoretical predictions of the normalized rotational friction coefficient (γ_r/γ_r^0) (black line) and translational friction coefficient $(\gamma_t^0/\gamma_t)^2$ (red line) of a CAP with *r* = 3.76 cm, as functions of obstacle area fraction ϕ. Inset: Theoretically predicted normalized diffusion coefficient D/D_0 versus ϕ, exhibiting a peak at ϕ = 0.70.

New reads:

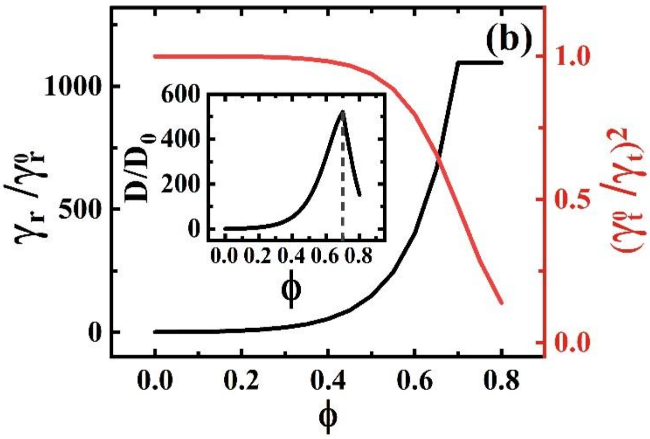

(b) The empirical predictions of the normalized rotational friction coefficient (γ_r/γ_r^0) (black line) and translational friction coefficient $(\gamma_t^0/\gamma_t)^2$ (red line) of a CABP with *r* = 3.76 cm, as functions of obstacle area fraction ϕ. Inset: The empirical predicted normalized diffusion coefficient D/D_0 versus ϕ, exhibiting a peak at ϕ = 0.70.

2. Page 6, right column, first paragraph

Following the sentence "On this basis, the theoretical prediction from Eq. (6), presented in the inset of Fig. 5(b), successfully reproduces the trends observed in both the experimental diffusion coefficient D/D_0 [blue triangles in Fig. 2(b)] and $v^2t_m/(v_0^2t_{tot})$ [blue triangles in Fig. 5(a)].", we added the following sentences: "The same empirical fitting functions and scaling analysis were applied to four additional CABPs with different orbital radii *r*, all of which show consistent agreement with the observed trends [Supplementary Material]."

Comment (17): The so-called prediction in Eq. (6) provides the behavior of the diffusion coefficient as the ratio of two frictions which are obtained by an empirical fitting. The great agreement in Fig 5c has some value, but provides somehow recursive information. Unless I am missing something.

Response (17): We thank the reviewer for this constructive suggestion. We agree that Eq. (6) expresses the diffusion coefficient as a ratio of two effective frictions that are both obtained from empirical fits. Consequently, the critical obstacle area fraction ϕ_c inferred from this empirical relation is not statistically independent of the quantities shown in Fig. 4, as they originate from the same experimental dataset.

The purpose of Fig. 5(c) was therefore to demonstrate that the value of ϕ_c inferred from the empirical relation is consistent with the obstacle fraction at which the diffusion coefficient reaches its maximum when calculated directly. This agreement supports the physical interpretation that the nonmonotonic diffusion of CABPs arises from the competition between enhanced directional persistence and suppressed migration velocity.

Nevertheless, we recognize that the original presentation may have obscured the degree of independence between the compared quantities. To avoid potential misunderstanding, we have revised Fig. 5(c) and modified the corresponding discussion in the updated manuscript.

Text changes:

1. Page 5, Fig. 5(c) and its caption

It was:

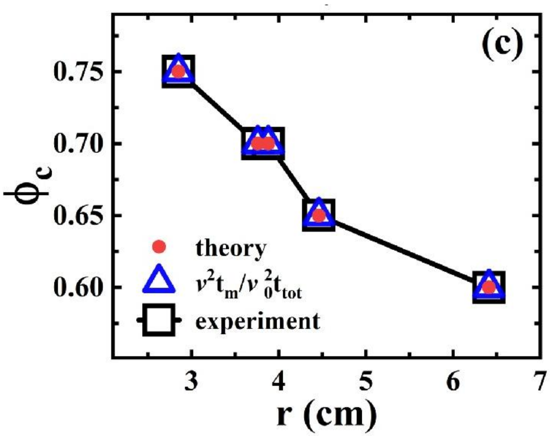

FIG. 5(c) Critical area fraction ϕ_c corresponding to the peak of experimentally measured D/D_0 (black squares), $v^2 t_m / v_0^2 t_{tot}$ (blue triangles), and theoretical prediction (red dots) for CAPs with different r.

New reads:

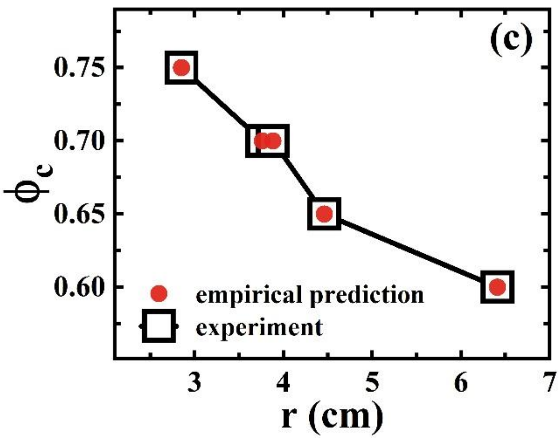

FIG. 5(c) Critical area fraction ϕ_c corresponding to the peak of experimentally measured D/D_0 (black squares) and empirical prediction (red dots) for CABPs with different r.

2. Page 4, right column, second paragraph

Delete the words: "Furthermore, both $v^2 t_m/(v_0^2 t_{tot})$ and the experimental diffusion coefficient D/D_0 attain their maxima at the same critical obstacle area fraction ϕ_c across different CAPs [Fig. 5(c)]."

3. Page 5, right column, second paragraph

It was: "Furthermore, the critical obstacle area fraction ϕ_c, obtained from all three independent measures, yields consistent values and systematically shifts toward smaller ϕ with increasing orbital radius r [Fig. 5(c)]."

New reads: "Furthermore, the critical obstacle area fraction ϕ_c, obtained from the experimental diffusion coefficient D/D_0 and the empirical prediction, yields consistent values and systematically shifts toward smaller ϕ with increasing orbital radius r [Fig. 5(c)]."

Comment (18): Although the whole manuscript focusses on chiral particles, Fig.3b implies that the effect of chirality plays a subdominant role. The importance of chirality is not so easy to appreciate since results are plotted in terms of D/D$_0$, where D$_0$ is different for different r.

Response (18): Figure 3(b) is intended to qualitatively illustrate the coexistence of two representative dynamical states of chiral active Brownian particles in obstacle environments across different particle sizes, following Ref. [Proc. Natl. Acad. Sci. USA 116, 22977 (2019)], rather than to highlight size-dependent differences in the dynamical behavior of CABPs. The apparent similarity of these states across particle sizes reflects a qualitative robustness rather than the absence of chirality effects. Importantly, chirality is essential for the emergence of these states. The coexistence of trapped and migratory dynamical states originates from the interactions between the chirality-driven circular motion and obstacles, which enables intermittent transitions between the two states.

The influence of chirality becomes more evident in the quantitative transport properties. As shown in Fig. 2(b), the diffusion curves for different orbital radii do not collapse, indicating a strong chirality dependence. The results were presented in terms of the normalized diffusivity D/D_0 in order to remove the contribution from single-particle free-space motion and isolate the effect of CABP–obstacle interactions. When the absolute diffusion coefficient D is plotted as a function of obstacle density [Fig. R16], the same nonmonotonic dependence is observed, while differences in magnitude arise both from the chirality-dependent free-space diffusivity D_0 and the CABP–obstacle interactions.

These points have been explicitly clarified in the revised manuscript to avoid potential misunderstanding.

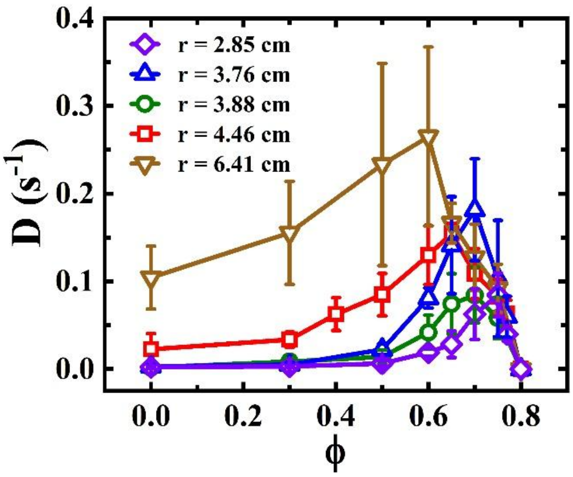

Fig. R16. The relation between ϕ and D for CAPs with r = 2.85, 3.76, 3.88, 4.46 and 6.41 cm.

Text changes:

Page 4, left column, at the end of second paragraph, we added the following words: "This universality does not diminish the fundamental role of chirality. Instead, the coexistence of trapped and migratory states, which underlies the observed dynamical heterogeneity, arises directly from particle chirality. The chirality-driven circular motion couples with deformable obstacles and induces intermittent transitions between these two states."

Comment (19): Is the transition between trapped and migration states similar to that described for self-propelled polymers in a complex media [PRL 134, 128303 (2025)].

Response (19): We thank the reviewer for pointing out this relevant connection. There is indeed a meaningful analogy between the trapped–migratory transition observed in our system of chiral active Brownian particles (CABPs) and the transition reported for self-propelled polymers in porous media [Phys. Rev. Lett. 134, 128303 (2025)].

In both cases, environmental complexity induces a transition between localized and extended modes of motion, resulting in enhanced long-range transport. In our system, deformable obstacles mediate a transition from a localized chiral orbital state to a directed migratory state, characterized by the migration time t_m and velocity v. In the polymer system, the porous medium drives a transition from caged dynamics within pores to reptation-like motion along curvilinear channels, governed by changes in polymer conformation (e.g., curling) and reorientation time. Despite distinct microscopic mechanisms, both systems share a common principle: the environment reshapes the intrinsic motility of active agents and intermittently promotes directed transport pathways. This analogy has been briefly discussed in the revised manuscript.

Text changes:

1. Page 1, right column, first paragraph

It was: "Notably, CAPs exhibit pronounced diffusion enhancement in disordered obstacles [4, 45–47], in stark contrast to the diffusion suppression typically observed for linear self-propelled particles under analogous conditions [48–51]."

New reads: "Notably, CABPs exhibit pronounced diffusion enhancement in disordered obstacles [4, 51-53], a similar counterintuitive enhancement has recently been observed for self-propelled polymer-like worms in disordered media [Phys. Rev. Lett. 134, 128303 (2025)], in stark contrast to the diffusion suppression typically observed for linear self-propelled particles under analogous conditions [55–58]."

Response to the comments from Reviewer 4

I co-reviewed this manuscript with one of the reviewers who provided the listed reports. This is part of the Communications Physics initiative to facilitate training in peer review and to provide appropriate recognition for Early Career Researchers who co-review manuscripts.

Response: We sincerely thank the reviewer for the positive assessment of our work. We have carefully revised the manuscript, added additional analyses as appropriate, and addressed all comments point by point.

Response to the Second Report of Reviewer #3

General comment:

The authors have submitted a revised and significantly enlarged version of the work, as can be seen by the pages extra of the main manuscript and 10 of the supplementary material. The answers to the comments were very complete and satisfactory. Overall, I think that the manuscript has largely gained in clarity and completeness, and it will become a reference work in the field. Therefore, I recommend it now for publication in for Communication Physics.

I would like still to add this few comments for the optional consideration of the authors.

Response： We sincerely thank the Reviewer for the careful evaluation, constructive suggestions, and positive assessment of our work. All comments have been carefully addressed, and the manuscript and Supplementary Material has been further revised accordingly. Detailed point-by-point responses are provided below.

Comment 1: Although complete, I found the answers to the comments excessively long and repetitive, and at some points they gave the impression that quite some AI was used.

Response 1: We thank the reviewer for this constructive comment. Considerable effort was made to ensure that the responses were clear, detailed, and logically structured. However, some parts became excessively long and repetitive, and we apologize for any inconvenience this may have caused. To improve readability and linguistic clarity, language-polishing tools (AI) were used in certain places. We greatly appreciate the reviewer's suggestions and will place greater emphasis on providing more concise, focused, and professional responses in the future work.

Comment 2: Regarding points 18 & 19. I am not completely convinced yet about the relevance of chirality in the coexistence of trapped and migratory dynamical states. Here, it can be true that the interactions between the chirality-driven circular motion and obstacles enables the transitions between the two states, but this could have as well happened due to the interaction of a random active motion and a disordered media.

Response 2: We thank the reviewer for this insightful comment. The coexistence of trapped and migratory dynamical states is not unique to chiral systems and has also been reported for self-propelled polymers in porous media [Phys. Rev. Lett. **134**, 128303 (2025)], where it arises from the interaction between the active motion and disordered media.

In the present work, the role of chirality lies in its influence on the transport response. For CABPs, the circular motion couples with obstacles, leading to a competition between enhanced motion collimation and suppressed migration velocity as the obstacle area fraction increases. This competition gives rises to the observed nonmonotonic diffusion enhancement, characterized by an initial increase followed by a decrease in diffusivity. Such nonmonotonic behavior was not reported in Ref. [Phys. Rev. Lett. **134**, 128303 (2025)]. To further examine the role of chirality, additional control experiments were performed using achiral particles (Fig. R1). In this case, the normalized diffusion coefficient D/D_0 decreases monotonically with increasing the obstacle area fraction ϕ. This comparison suggests that while state coexistence may occur in different active systems, the nonmonotonic diffusion enhancement observed here is closely associated with particle chirality. The corresponding clarification and Fig. R1 have been added to the revised manuscript and the Supplementary Material.

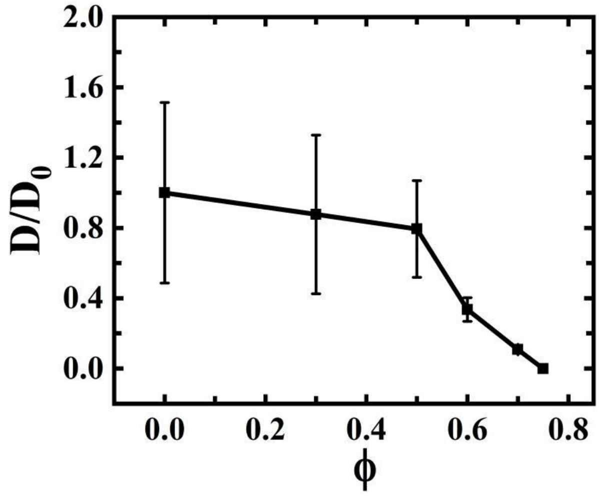

Fig. R1. Normalized diffusion coefficient D/D_0 of achiral particles as a function of obstacle area fraction ϕ.

Text changes:

1. Page 3, left column, first paragraph

It was: "Additional control experiments varying obstacle size, softness, and confinement geometry consistently confirm the robustness of this nonmonotonic diffusion behavior [Supplementary Material]."

Now reads: "Additional control experiments varying obstacle size, softness, and confinement geometry consistently confirm the robustness of this nonmonotonic diffusion behavior of CABPs [Supplementary Note 1-3], whereas no such nonmonotonic behavior is observed for achiral particle [Supplementary Note 4]."

Comment 3: The authors adapt the effective diffusion coefficient of CABP from the literature and apply it to the angular MSD they measure. However, it is not quite clear how they can adapt the 2D result for the CABP to their 1D case, since, e.g., the dimensions of Eq. (3) is not 1/s but cm^2/s, which cannot be consistent with the MSD definition. The authors should verify that the omission of the radial coordinate here is consistent.

Response 3: We thank the reviewer for this constructive comment. In the annular channel geometry, CABP dynamics are quantified using the angular coordinate, so that transport is effectively one-dimensional along the azimuthal direction with periodic boundary conditions. Over the explored range of obstacle area fraction ϕ, the mean radial coordinate of the five CABPs remains approximately constant, as shown in Fig. R2(a). This allows radial fluctuations to be neglected and transport to be characterized by the angular diffusion coefficient. Accordingly, the effective diffusion coefficient adapted from the literature is applied to the angular MSD and converted to a physical diffusivity through the mean radial coordinate, yielding the correct physical dimension and allowing direct comparison with the conventional translational diffusion coefficient.

To further validate this approach, the normalized two-dimensional translational diffusion coefficient D_t/D_t^0 was independently measured at different ϕ [R2(b)]. Its dependence on ϕ closely matches that of the normalized angular diffusion coefficient D/D_0, including identical peak positions. This agreement confirms that the 2D effective diffusion framework captures the essential transport behavior in our system and justifies its application to the angular MSD analysis. Corresponding clarifications and Fig. R2 have been added to the revised manuscript and the Supplementary Material.

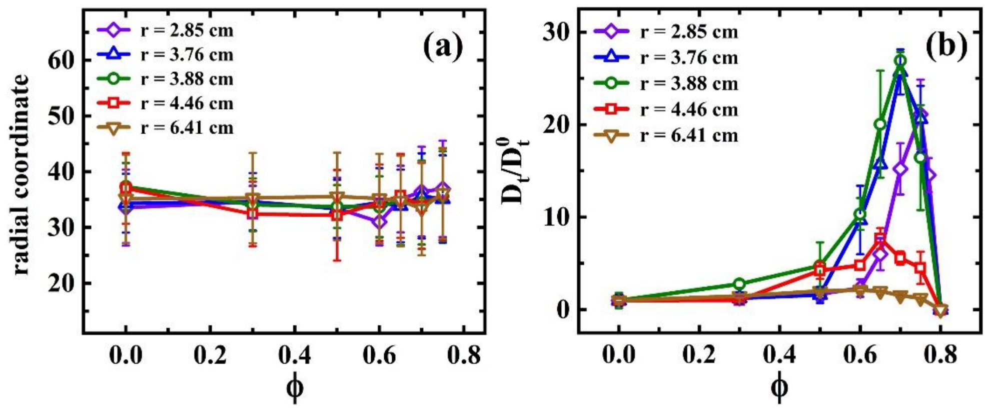

Fig. R2. (a) Mean radial coordinate of five CABPs as a function of obstacle area fraction ϕ. (b) Normalized translational diffusion coefficient D_t/D_t^0 of five CABPs versus ϕ.

Text changes:

1. Page 5, right column, third paragraph

It was: "In the annular channel geometry, CABP motion along the azimuthal direction θ is effectively unconfined and experiences periodic boundary conditions. Consequently, the measured angular displacement $\Delta\theta$ can exceed 2π. Under obstacle-free conditions, the effective diffusion coefficient of a CABP can therefore be expressed theoretically as [36, 62, 63] ……."

Now reads: "In the annular channel geometry, CABP motion along the azimuthal direction θ is effectively unconfined and experiences periodic boundary conditions, allowing the angular displacement $\Delta\theta$ to exceed 2π. Across the explored obstacle area fraction ϕ, the mean radial coordinate remains approximately constant [Supplementary Note 9], indicating that radial fluctuations have a negligible influence on longtime transport. Diffusion can therefore be characterized by the angular diffusion coefficient, which can be converted to the corresponding translational diffusivity through the mean radial coordinate. Under obstacle-free conditions, the effective diffusion coefficient of a CABP can be expressed theoretically as [36, 62, 63] ……."

Comment 4: Regarding point 7 of referee 1. To extrapolate the definition of temperature from micrometer systems to this centimeter systems is not completely straightforward, and that the use of other concepts like particle persistence time might be more appropriate. Equations (4) to (7) make use of microscopic definitions, including temperature, which cancels out in the end in Eq. (8).

Response 4: We thank the reviewer for this helpful suggestion. We agree that extending the definition of temperature from micrometer systems to centimeter systems is not completely straightforward. To avoid potential ambiguity, the definition of temperature has been removed in the revised manuscript.

The formulation is now expressed in terms of the persistence time $\tau_r = 1/D_r$ [Phys. Rev. E **82**, 015304 (2010)]. In the Hexbug systems, the rotational diffusion coefficient follows $D_r \propto \gamma_r^{-1}$ and can be written as $D_r = E_{eff}\gamma_r^{-1}$ [arXiv:2403.02569], where the proportionality factor E_{eff} is related to the effective thermal energy. E_{eff} can reasonably be assumed to remain approximately unchanged with and without obstacles since the energy input originates from the Hexbug itself. Equations (4) to (7) have been reorganized accordingly to ensure internal consistency without reliance on microscopic temperature-based definitions. Corresponding clarifications have been added to the revised manuscript.

Text change:

Page 5, right column, third paragraph

It was: "Under obstacle-free conditions, the effective diffusion coefficient of a CABP can therefore be expressed theoretically as [36, 62, 63],

$$D = D_t^T + \frac{v^2\tau_r}{2[1+(\omega\tau_r)^2]}. \quad (3)$$

For a CABP moving in obstacle-free space, the thermal translational diffusion coefficient is given by $D_t^T = k_B T/\gamma_t^0$. The rotational relaxation time (i.e., the persistence time) is defined as $\tau_r = 1/D_r = \gamma_r^0/(k_B T)$, where D_r is the rotational diffusion coefficient extracted from the mean-squared angular displacement (MSAD) or orientation autocorrelation [64, 65]. The translational and angular velocity are $v_0 = F_d/\gamma_t^0$ and $\omega_0 = T_d/\gamma_r^0$, respectively, with γ_t^0 and γ_r^0 being the translational and rotational friction coefficients in obstacle-free space, and F_d and T_d the driving force and torque acting on the particle.

Accordingly, the effective diffusion coefficients in obstacle-free space can be approximated as

$$D_0 = k_B T/\gamma_t^0 + \frac{{F_d}^2\gamma_r^0/{\gamma_t^0}^2}{2k_B T\left[1+(\frac{T_d}{k_B T})^2\right]} \quad (4)$$

The environment with increasing obstacle area fraction ϕ simultaneously modifies translational and rotational dynamics. Frequent collisions suppress the migration speed, thereby enhancing the effective translational friction $\gamma_t(\phi)$, while the obstacle-induced alignment enhances orientational persistence, effectively reducing the rotational diffusion coefficient and leading to an increased effective rotational friction $\gamma_r(\phi)$. These effects motivate us to treat both friction coefficients as ϕ-dependent. Experimentally, they are captured by the empirical relations $\gamma_r(\phi) \propto t_m/t_{tot}$ and $\gamma_t(\phi) \propto v_0/v$, which quantify the enhancement of directional persistence and the suppression of migration speed, respectively. By substituting these relations into Eq. (4) yields the generalized diffusion coefficient in obstacle-rich environments,

$$D = k_B T/\gamma_t(\phi) + \frac{{F_d}^2 \gamma_r(\phi)/\gamma_t(\phi)^2}{2k_B T\left[1+(\frac{T_d}{k_B T})^2\right]}. \tag{5}$$

Since the thermal translational term $D_t^T = k_B T/\gamma_t(\phi)$ is negligibly compared with the activity-induced contribution, the effective diffusion coefficients of particles in the presence and absence of obstacles can be approximated as

$$D \approx \frac{{F_d}^2 \gamma_r(\phi)/\gamma_t(\phi)^2}{2k_B T\left[1+(\frac{T_d}{k_B T})^2\right]}, \tag{6}$$

$$D_0 \approx \frac{{F_d}^2 \gamma_r^0/{\gamma_t^0}^2}{2k_B T\left[1+(\frac{T_d}{k_B T})^2\right]}. \tag{7}$$

Consequently, the normalized diffusion coefficient becomes

$$\frac{D}{D_0} = \frac{\gamma_r(\phi){\gamma_t^0}^2}{\gamma_t^2(\phi)\gamma_r^0}. \tag{8}$$

”

Now reads: “Under obstacle-free conditions, the effective diffusion coefficient of a CABP can be expressed theoretically as [36, 62, 63],

$$D_0 = D_t^T + \frac{v_0^2 \tau_r}{2[1+(\omega_0 \tau_r)^2]}. \tag{3}$$

Since the thermal contribution D_t^T is negligibly compared with the activity-induced term, the effective diffusion coefficient can be approximated as

$$D_0 \approx \frac{v_0^2 \tau_r}{2[1+(\omega_0 \tau_r)^2]}. \tag{4}$$

Here $v_0 = F_d/\gamma_t^0$ and $\omega_0 = T_d/\gamma_r^0$, where γ_t^0 and γ_r^0 denote the translational and rotational friction coefficients in obstacle-free space, while F_d and T_d are the driving force and torque acting on the particle. The persistence time is defined as $\tau_r = 1/D_r$ [62], where D_r is obtained from the mean-squared angular displacement or the orientation autocorrelation [64, 65]. For the Hexbug systems, $D_r \propto \gamma_r^{-1}$ and can be written as $D_r = E_{eff}\gamma_r^{-1}$, where the proportionality factor E_{eff} is related to the effective thermal energy. E_{eff} can be reasonably assumed to remain unchanged with and without obstacles since the energy input originates from the Hexbug itself.

In obstacle-rich environments, increasing obstacle area fraction ϕ modifies both translational and rotational dynamics. Frequent collisions reduce the migration speed, effectively increasing the translational friction $\gamma_t(\phi)$, while obstacle-induced alignment enhances orientational persistence, thereby reducing the rotational diffusion coefficient and increasing the effective rotational friction $\gamma_r(\phi)$. Both friction coefficients are therefore treated as ϕ-dependent. Experimentally, they are captured by the empirical relations $\gamma_r(\phi) \propto t_m/t_{tot}$ and $\gamma_t(\phi) \propto v_0/v$, which quantify the enhancement of directional persistence and the suppression of migration speed, respectively. Substituting these relations into Eq. (4) yields the effective diffusion coefficient for obstacle-free and obstacle-rich environments,

$$D_0 = \frac{{F_d}^2 \gamma_r^0}{2E_{eff}(\gamma_t^0)^2[1+({E_{eff}}^{-1}T_d)^2]}, \tag{5}$$

$$D = \frac{{F_d}^2 \gamma_r(\phi)}{2E_{eff}\gamma_t^2(\phi)[1+({E_{eff}}^{-1}T_d)^2]}, \tag{6}$$

leading to the normalized diffusion coefficient

$$\frac{D}{D_0} = \frac{\gamma_r(\phi)(\gamma_t^0)^2}{\gamma_t^2(\phi)\gamma_r^0}. \tag{7}$$

”